Atmos. Chem. Phys. Discuss., https://doi.org/10.5194/acp-2017-747
Manuscript under review for journal Atmos. Chem. Phys.
Discussion started: 12 October 2017

Atmospheric Chemistry and Physics Discussions

Revisiting the contribution of land transport and shipping emissions to tropospheric ozone

Mariano Mertens[1], Volker Grewe[1a], Vanessa S. Rieger[1a], and Patrick Jöckel[1]

[1]Deutsches Zentrum für Luft- und Raumfahrt, Institut für Physik der Atmosphäre, Oberpfaffenhofen, Germany
[a]also at: Delft University of Technology, Aerospace Engineering, Section Aircraft Noise and Climate Effects, Delft, the Netherlands

Correspondence to: Mariano Mertens (mariano.mertens@dlr.de)

Abstract. We quantify the contribution of land transport and shipping emissions to tropospheric ozone for the first time with a chemistry-climate model including an advanced tagging method, which considers not only the emissions of NO_x (NO and NO_2), CO or non-methane hydrocarbons ($NMHC$) separately but the competing effects of all relevant ozone precursors. For summer conditions a contribution of land transport emissions to ground level ozone of up to 18 % in North America and South Europe is estimated, which corresponds to 12 $\mathrm{nmol\ mol^{-1}}$ and 10 $\mathrm{nmol\ mol^{-1}}$, respectively. The simulation results indicate a contribution of shipping emissions to ground level ozone during summer in the order of up to 30 % in the Northern Pacific (up to 12 $\mathrm{nmol\ mol^{-1}}$) and 20 % in the Northern Atlantic (12 $\mathrm{nmol\ mol^{-1}}$). To put these estimates in the context of literature values, we review previous studies. Most of them used the perturbation approach, in which the results from two simulations, one with all emissions and one with changed emissions for the source of interest, are compared. The comparison shows that the results strongly depend on the chosen methodology (tagging or perturbation method) and on the strength of the perturbation. A more in-depth analysis for the land transport emissions reveals that the two approaches give different results particularly in regions with large emissions (up to a factor of four for Europe). With respect to the contribution of land transport and ship traffic emissions to the tropospheric ozone burden we quantified values of 8 % and 6 % for the land transport and shipping emissions, respectively. Overall, the emissions from land transport contribute to around 20 % of the net ozone production near the source regions, while shipping emissions contribute up to 52 % to the net ozone production in the Northern Pacific. Our estimates of the radiative ozone forcing due to emissions of land transport and shipping emissions are 92 $\mathrm{mW\ m^{-2}}$ and 62 $\mathrm{mW\ m^{-2}}$, respectively. Again these results are larger by a factor of 2–3 compared to previous studies using the perturbation approach, but largely agree with previous studies which investigated the difference between the tagging and the perturbation method. Overall our results highlight the importance of differing between the perturbation and the tagging approach, as they answer two different questions. We argue that only the tagging approach can estimate the contribution of emissions, while only the perturbation approach investigates the effect of an emission change. To effectively asses mitigation options both approaches should be combined.

Atmos. Chem. Phys. Discuss., https://doi.org/10.5194/acp-2017-747
Manuscript under review for journal Atmos. Chem. Phys.
Discussion started: 12 October 2017

Atmospheric Chemistry and Physics Discussions

1 Introduction

Ozone in the troposphere has several well known effects: it contributes to global warming due to its radiative properties (e.g. Stevenson et al., 2006; Myhre et al., 2013), and large concentrations of ozone are harmful to humans and to plants (e.g. World Health Organization, 2003; Fowler et al., 2009). In addition, ozone is an important source for the OH radical, which controls the cleansing capacity of the troposphere (e.g. the lifetime of methane, Naik et al., 2013). Due to these different effects ozone is a central species of atmospheric chemistry (Monks et al., 2015).

Two important sources of ozone exist in the troposphere – the downward transport from the stratosphere and the in-situ production from precursors emissions (e.g. Lelieveld and Dentener, 2000; Grewe, 2004). The most important precursors of ozone are carbon monoxide (CO), methane (CH_4), non-methane hydrocarbons (NMHC) and nitrogen oxides (NO_x=NO+NO_2, e.g. Haagen-Smit, 1952; Crutzen, 1974; Monks, 2005). These precursors have anthropogenic as well as natural sources. Important natural sources of NMHCs are biogenic emissions (e.g. Guenther et al., 1995), while NO_x is emitted by lightning (e.g. Schumann and Huntrieser, 2007) and soil (e.g. Yienger and Levy, 1995; Vinken et al., 2014). anthropogenic sources of ozone precursors, on the other hand, include emissions from industry, land transport (containing the sectors road traffic, inland navigation and railways, e.g. Uherek et al., 2010) and shipping (e.g. Eyring et al., 2010).

To define mitigation strategies or to calculate climate impacts, it is important to know which emission source contributes to what extent to the ozone concentration. Because of the non-linearity of the O_3 chemistry it is not possible to calculate the amount of produced ozone directly from the amount of the emissions. Instead, the contribution of different sources needs to be estimated by means of simulations with advanced models, either chemistry transport models or chemistry climate models. However, only the latter allow to directly quantify the impacts of the chemical species on the climate.

Many of such investigations have been performed in the past to estimate the contribution of road traffic (but not the total land transport effect, e.g., Granier and Brasseur, 2003; Niemeier et al., 2006; Matthes et al., 2007; Hoor et al., 2009; Koffi et al., 2010; Dahlmann et al., 2011; Grewe et al., 2012) and shipping (e.g. Lawrence and Crutzen, 1999; Eyring et al., 2007; Hoor et al., 2009; Koffi et al., 2010; Holmes et al., 2014) emissions to tropospheric ozone on the global scale. Typically two different approaches are used in such studies – the perturbation and the tagging approach. Most of previous studies used the perturbation approach in which the results from a reference simulation including all emission sources with the results of a perturbed simulation with changed emissions of a specific source are compared. In the tagging approach additional diagnostic species are introduced which follows the reaction pathways of the emissions from different sources (e.g. Lelieveld and Dentener, 2000; Grewe, 2004; Emmons et al., 2010; Butler et al., 2011; Grewe et al., 2012; Emmons et al., 2012). Assuming a linear system both approaches lead to identical answers (e.g. Grewe et al., 2010). In case of a non-linear system (as the O_3 chemistry) both methods lead to different results as they answer different questions. The perturbation approach addresses the question: 'What is the change in ozone, if the emissions of the source of interest are changed?' (e.g. Wu et al., 2009; Grewe et al., 2010). Accordingly the perturbation approach calculates the impact of e.g. land transport emissions on tropospheric ozone.

To investigate the contribution (also called source attribution) the so-called tagging approach is much better suited. It has been shown that the contributions estimated by the tagging approach are larger compared to the impacts calculated using the

Atmos. Chem. Phys. Discuss., https://doi.org/10.5194/acp-2017-747
Manuscript under review for journal Atmos. Chem. Phys.
Discussion started: 12 October 2017

Atmospheric Chemistry and Physics Discussions

perturbation approach (e.g. Grewe et al., 2012; Emmons et al., 2012; Grewe et al., 2017). However, so far no study investigated the contribution of land transport and shipping emissions in detail using a tagging approach. In addition, our approach tags for the first time not only NO_x and NMHC individually, but both ozone precursors concurrently (Grewe et al., 2017).

The goal of the present study is twofold: First we review estimates of the contribution/impact of land transport/road traffic and ship traffic emissions on tropospheric ozone and the resulting radiative forcing. Second we present new results using a detailed tagging method, which has so far not been used to investigate the contribution of land transport and shipping emissions. This includes a comparison of the tagging and the perturbation method. Further we provide detailed information about the influence of the emissions from land transport and shipping on the tropospheric ozone budget.

The paper is organised as follows: In Sect. 2 we give an overview of the used model system and describe the applied set-up. In Sect. 3 we analyse the simulation results with respect to the contribution of land transport and shipping emissions to ground level ozone including a detailed overview and discussion of results from previous studies. In Sect. 4 we compare results using the perturbation and the tagging approach in more detail. Section 5 gives more detailed insights into the tropospheric ozone budget. Finally, Sect. 6 analyses the contribution of the land transport and shipping emissions to radiative forcing due to ozone.

2 Model description and set-up

We applied the ECHAM/MESSy Atmospheric Chemistry (EMAC) chemistry-climate model (Jöckel et al., 2006, 2010, 2016) equipped with the TAGGING technique described by Grewe et al. (2017). EMAC uses the second version of the Modular Earth Submodel System (MESSy2) to link multi-institutional computer codes. The core atmospheric model is the 5th generation European Centre Hamburg general circulation model (ECHAM5 Roeckner et al., 2006). For the present study we applied EMAC (ECHAM5 version 5.3.02, MESSy version 2.52) in the T42L90MA-resolution, i.e. with a spherical truncation of T42 (corresponding to a quadratic Gaussian grid of approx. 2.8 by 2.8 degrees in latitude and longitude) with 90 vertical hybrid pressure levels up to 0.01 hPa. The simulation set-up is almost identical to the one of the simulation *RC1SD-base-10a* described in detail by Jöckel et al. (2016) alongside with an evaluation of the resulting model simulation. Therefore, we describe only the most important details and differences. A comparison with the results of the simulation presented here and the *RC1SD-base-10a* is part of the Supplement of the present manuscript.

The chosen simulation period covers the years 2004 to 2010. The years 2004–2005 serve as spin-up, while the years 2006–2010 are analysed. Initial conditions for the trace gas distribution were taken from the *RC1SD-base-10a* simulation (Jöckel et al., 2016). Lightning NO_x is parameterised after Grewe et al. (2002) with global total emissions of $\approx 4.5\ \mathrm{Tg(N)\ a^{-1}}$. Emissions of NO_x from soil and biogenic C_5H_8 emissions were calculated using the MESSy submodel ONEMIS (Kerkweg et al., 2006), using parameterisations based on Yienger and Levy (1995) for soil-NO_x and Guenther et al. (1995) for biogenic C_5H_8. The applied gas phase mechanism in MECCA (Sander et al., 2011) incorporates the chemistry of ozone, methane and odd nitrogen. Alkanes and Alkenes are considered up to C4, while the oxidation of C_5H_8 and some non-methane hydrocarbons (NMHCs) are described with the Mainz Isopren Mechanism version 1 (von Kuhlmann et al., 2004). Further, heterogeneous

Atmos. Chem. Phys. Discuss., https://doi.org/10.5194/acp-2017-747
Manuscript under review for journal Atmos. Chem. Phys.
Discussion started: 12 October 2017

Atmospheric Chemistry and Physics Discussions

reactions in the stratosphere (submodel MSBM, Jöckel et al., 2010) as well as aqueous phase chemistry and scavanging (SCAV, Tost et al., 2006) are included.

EMAC is 'nudged' by Newtonian relaxation of temperature, divergence, vorticity and the logarithm of surface pressure (Jöckel et al., 2006) towards ERA-Interim (Dee et al., 2011) reanalysis data. Also the the sea surface temperature and sea ice coverage are prescribed as transient time-series from ERA-Interim too. To allow for identical meteorological conditions in sensitivity experiments with changed emissions, the quasi chemistry transport model mode (QCTM-mode, Deckert et al., 2011) of EMAC was used. In this mode, climatologies of the radiative active trace gases are prescribed for the calculation of the radiation. Further, climatologies are used for processes which couple the chemistry and the hydrological cycle. The applied climatologies are monthly average values taken from the *RC1SD-base-10a* simulation.

The tagging is performed using the MESSy TAGGING submodul described in detail by Grewe et al. (2017). This tagging method is an accounting system following the relevant reaction pathways and applies the generalized tagging method introduced by Grewe (2013). This method diagnoses the contributions of different categories to the regarded species without influencing the full chemistry. A prerequisite for this method is a complete decomposition of the source terms, e.g. emissions, of the regarded species in N unique categories. As a consequence of the complete decomposition, the sum of the contributions of all tagged categories of one specie equals the total concentration of this specie (i.e. the budget is closed):

$$\sum_{\mathrm{tag}=1}^{N} \mathrm{O_3^{tag}} \quad = \quad \mathrm{O_3}. \tag{1}$$

As an example of this method consider the production of $\mathrm{O_3}$ by the reaction of NO with an organic peroxy radical ($\mathrm{RO_2}$) to $\mathrm{NO_2}$ and the organic oxy radical (RO):

$$\mathrm{NO + RO_2 \longrightarrow NO_2 + RO}. \tag{R1}$$

For this reaction the tagging approach leads to the following fractional apportionment (c.f. Eq. 13 and 14 in Grewe et al., 2017, for a detailed example):

$$\mathrm{P_{R1}^{tag}} \quad = \tfrac{1}{2}\mathrm{P_{R1}}\left(\frac{\mathrm{NO_y^{tag}}}{\mathrm{NO_y}} + \frac{\mathrm{NMHC^{tag}}}{\mathrm{NMHC}}\right). \tag{2}$$

In this case the variables marked with $^{\mathrm{tag}}$ represent the tagged production rate of $\mathrm{O_3}$ by reaction R1 ($\mathrm{P_{R1}}$) as well as the tagged families of $\mathrm{NO_y}$ and NMHC (details given below) of one individual category (e.g. land transport). Accordingly the fractional apportionment is inherent to the method based on a combinatorial approach, which decomposes every regarded reaction into all possible combinations of reacting tagged species. This takes into account the specific reaction rate constant from the full chemistry scheme (implicitly by the production and loss rates from the chemistry solver).

The applied method considers ten categories (detailed definition is given in Table 1). To minimize the needed amount of memory and computational performance, not every individual specie is tagged. Instead a family concept is chosen. The

Atmos. Chem. Phys. Discuss., https://doi.org/10.5194/acp-2017-747
Manuscript under review for journal Atmos. Chem. Phys.
Discussion started: 12 October 2017

Atmospheric Chemistry and Physics Discussions

following families are taking into account: O_3, NO_y, PAN, NMHC and CO. Additionally, OH and HO_2 are tagged by a steady state approach.

As anthropogenic emissions inventory we chose the MACCity emission inventory (Granier et al., 2011), which follows the RCP8.5 scenario (Riahi et al., 2007, 2011) for the analysed period. The monthly varying anthropogenic emissions are represented on a grid with $0.5°$ x $0.5°$ spatial resolution. The geographical distribution of the land transport (containing road traffic, inland navigation and railways) and the shipping sector are shown in Fig. 1. Additionally, the total emissions of CO, NO_x and NMHCs of the most important emission sectors are given in Table 2.

We conducted three different simulations: one with all emissions (*BASE*), one with a 5 % decrease of the land transport emissions of NO_x, CO and NMHCs (*LTRA95*), and one with a 5 % decrease of the shipping emissions of NO_x, CO and NMHCs (*SHIP95*). All three simulations were equipped with the full tagging diagnostics. To quantify the contribution of the emission sources the tagging results of the *BASE* simulation are used. The simulations with a decrease of the land transport and shipping emissions were performed to allow for a direct comparison between the tagging and the perturbation method. The additional tagging diagnostics in the perturbed simulations allow for a more detailed investigations in the change of the ozone production (see Sect. 4).

In the present study we focus on the source regions of land transport and shipping emissions. Therefore we use the same geographical regions as defined by Righi et al. (2013) to investigate the contribution these emissions. The regions are Europe (EU), North America (NA) and Southeast Asia (SEA) for land transport, and North Atlantic Ocean (NAO), Indian Ocean (IO) and North Pacific Ocean (NPO) for the shipping emissions.

3 Contribution to ground level ozone

First, we analyse the absolute amount of O_3 produced by land transport (tra) and ship (shp) exhaust as analysed with the Tagging method. We denote absolute contributions diagnosed with the tagging method as O_3^{tra} and O_3^{shp}, respectively. Additionally we indicate also the relative contribution of O_3^{tra} and O_3^{shp} to near ground level O_3. For all quantities multi-annual, seasonal average values for December–Februar (DJF) as well as June–August (JJA) for the years 2006–2010 (for DJF starting with December 2005) were computed.

3.1 Land transport

Figure 2a and Fig. 2b show the seasonal average values of O_3^{tra} for DJF and JJA . The maximum absolute contribution for each hemisphere are simulated during local summer conditions when the photochemistry is most effective. Most geographical locations of these maxima correspond to the regions with the largest land transport emissions. The largest absolute contributions of 8–14 $nmol\ mol^{-1}$ are simulated during JJA on the Northern Hemisphere in North America (8–12 $nmol\ mol^{-1}$), Southern Europe (8–10 $nmol\ mol^{-1}$), the Arabian Pensinsula (12–14 $nmol\ mol^{-1}$), India (8–10 $nmol\ mol^{-1}$) and Southeast Asia (6–10 $nmol\ mol^{-1}$). In Asia the largest values are simulated around the Korean Peninsula rather than in China. This lower contribution of land transport emissions in China compared to Europe or North America is mainly caused by a much larger

Atmos. Chem. Phys. Discuss., https://doi.org/10.5194/acp-2017-747
Manuscript under review for journal Atmos. Chem. Phys.
Discussion started: 12 October 2017

Atmospheric Chemistry and Physics Discussions

fraction of other anthropogenic emissions (e.g. industry and households) compared to land transport emissions (e.g. Righi et al., 2013). Accordingly much more O_3 is produced in China by other anthropogenic emissions compared to land transport. The local maxima (4–6 $\mathrm{nmol\ mol^{-1}}$) on the Southern Hemisphere are simulated during DJF, when the photochemistry is most active. These maxima are located in South America and South Africa. Corresponding the regions with the largest land transport emissions on the Southern hemisphere (cf. Fig. 1).

The relative contribution of O_3^{tra} to near ground level O_3 is depicted in Fig. 2c and Fig. 2d. Values of 14–16 % are simulated during DJF around the source regions on the Southern Hemisphere, but the absolute values on the Southern Hemisphere are lower compared to the Northern Hemisphere. The simulated relative contributions on the Northern Hemisphere during DJF is around 10 %. Only around the Arabian Peninsula values of 14–16 % are found. During JJA, these maxima increase to 14–18 % over North America and 12–16 % for the other hotspot regions on the Northern Hemisphere. One important reason for the change of the contribution from DJF to JJA (on the Northern Hemisphere) is the strong seasonal cycle of the anthropogenic non-traffic sector in our applied emission inventory, showing large emissions during winter and lower emissions during summer. This leads to larger contributions of the anthropogenic non-traffic category during DJF compared to JJA.

To review estimates of the impact/contribution of previous studies and to compare the new results with previous values, Table 3 summarises the amount of emissions as well as reported impacts/contributions of road traffic emissions from previous studies. So far, only the effects of road traffic emissions alone and not the total effect of land transport emissions have been investigated. With respect to the ozone precursors road traffic emissions are the largest contributor to the land transport sector. The contributions of inland navigation and railways are smaller than the uncertainties of the road traffic emissions. Therefore we argue that our results of the land transport sector can be compared with previous studies considering only road traffic emissions (cf. also the amount of applied emissions in different studies in Table 3). In general, we are focussing on global studies only. Regional effects of road traffic emissions have been investigated too (e.g. Reis et al., 2000; Tagaris et al., 2015; Hendricks et al., 2017), but because of the coarse resolution of global models a quantitative comparison between findings of regional studies with these global studies is not straightforward and probably not meaningful. Please note that we provide in Table 3 the values of the present study only for July to allow for a better comparability. In addition the impact of the land transport emissions were calculated by with the results of the unperturbed and perturbed simulation (*BASE* minus *LTRA95*) which is scaled by 20 to estimate a 100 % perturbation. Figures showing the contribution/impact for the results of the present study are part of the Supplement.

Previously, the impact of road traffic emissions on ozone concentration has been investigated mainly using 100 % and 5 % perturbation approaches. Most previous studies applied similar amounts of road traffic emissions as the present study used for land transport emissions (9–10 $\mathrm{Tg\ a^{-1}}$). The fraction of NO_x emissions from road traffic compared to all emissions was largest in the studies of Granier and Brasseur (2003), Niemeier et al. (2006) and Matthes et al. (2007). These studies also applied the largest CO and NMHC emissions, while the individual fractions vary across the studies.

In general, the results of all considered studies can be separated into three groups: (1) The largest values are reported by the present study (using the tagging method) as well as by Niemeier et al. (2006). (2) Slightly lower values are given by Granier and Brasseur (2003) and Matthes et al. (2007), while (3) Hoor et al. (2009) and Koffi et al. (2010) report the lowest impact.

These studies, however, differ not only in the emission inventories and models used, but also in the methods. The lowest values are in general reported by studies using the 5 % perturbation (scaled to 100 %), which is confirmed by our results using the same method. However, compared to other 5 % studies our results show, especially for NA, slightly larger values. This might be caused by a different geographical distribution and larger CO and NMHC emissions in our applied emission inventory. Further, differences in the atmospheric composition as simulated by the different models can influence the production rates of ozone, which might contribute to the differences of the simulated impacts.

The comparison of our results using the 5 % perturbation approach and the results using the tagging approach clearly confirms the known underestimation of the contribution by the perturbation approach (e.g. Wu et al., 2009; Grewe et al., 2010; Emmons et al., 2012; Grewe et al., 2012, 2017). Depending on the region, we find a difference of up to a factor of 4. The reason for this difference is investigated in more detail in Sect. 4.

Granier and Brasseur (2003), Niemeier et al. (2006) and Matthes et al. (2007), however, also used a perturbation approach, but report values, which are more similar to our estimate using the tagging method. This is likely caused by the larger emissions applied in these studies compared to all other studies. Accordingly, the contribution of the road traffic emissions is underestimated by the perturbation method, but the larger emissions (and fraction) of the road traffic category lead to results, which are similar as estimated by the tagging method with smaller emissions. Of course also other factors, like differences between the models, chemical mechanisms, geographical distribution, and different seasonal cycles of the emissions can contribute to differences between the studies. The influence of these factors, however, is difficult to reveal.

3.2 Ship traffic

The absolute contribution of O_3^{shp} are shown in Fig. 3a and Fig. 3b. Similar to the shipping emissions (cf. Fig. 1), O_3^{shp} shows a strong North-South gradient. The maximum values in the Northern Hemisphere are located between 20°–30° N during DJF ($\approx$ 6 nmol mol^{-1}). These maxima move northwards during summer and increase in magnitude (10–12 nmol mol^{-1}). This shift is caused by the increase in the photochemical activity in the Northern hemisphere during summer. Most shipping emissions are located north of 30° N (see Fig. 1). With increasing ozone production during spring and summer more O_3^{shp} near the regions with the largest emissions are formed, compared to the regions of 20–30° N.

The largest values of the relative contribution of O_3^{shp} during DJF are around 14 % and are co-located with the regions of the largest values of O_3^{shp} (Fig. 3c). The maxima of the contribution increase during JJA to around 30 % in the Northwestern Pacific, while the values in the Northeastern Pacific are around 18–22 %. In the Northern Atlantic maximum contributions of 20 % are simulated (Fig. 3d).

Table 4 summarises emissions and results of previous studies. In general most studies used similar global NO_x shipping emissions of around 4 Tg(N) a^{-1}. The largest impact/contribution of shipping emissions is limited to distinct areas within the investigated geographical regions. Therefore the range of the given contributions/impacts within the geographical regions is large. The displacement between the regions of emissions and largest ozone production is well known (e.g. Endresen et al., 2003; Eyring et al., 2007) and mainly caused by complex interplay between NO_x emissions, transport of precursors and ozone production.

Atmos. Chem. Phys. Discuss., https://doi.org/10.5194/acp-2017-747
Manuscript under review for journal Atmos. Chem. Phys.
Discussion started: 12 October 2017

Similar as discussed for the impact/contribution of land transport emissions, there is a large discrepancy between the results using the 100 % and the 5 % perturbation method. The studies using the 100 % method report impacts in the Atlantic and the Pacific in the range of 4–11 $\mathrm{nmol\ mol^{-1}}$ (corresponding to 12–40 %). In general the previous studies report larger impacts in the Pacific compared to the Atlantic. Only Eyring et al. (2007) reported a larger perturbation in the Northern Atlantic compared to the Pacific, which can most likely be attributed to differences in the emission inventories, as Eyring et al. (2007) applied lower emissions in the Northern Pacific compared to the Northern Atlantic.

Hoor et al. (2009) and Koffi et al. (2010) report absolute impacts (5 % perturbation) in the range of 2–6 $\mathrm{nmol\ mol^{-1}}$. Our model results using a 5 % perturbation suggest somewhat larger impacts of around 2–8 $\mathrm{nmol\ mol^{-1}}$ (10–22 %) in the Atlantic and Pacific. Most likely this difference can be attributed to different shipping emissions applied.

The absolute contributions diagnosed using the tagging approach are larger and in the range of 3–11 $\mathrm{nmol\ mol^{-1}}$ (relative contribution: 10–33 %) in the Atlantic and Pacific. These contributions are at the lower end of the contributions reported by the studies using the 100 % approach. Compared to these studies, however, we applied the largest shipping emissions. Accordingly, a larger contribution compared to other studies can be expected. As the used models and emission inventories in all studies are very different we can only speculate about possible reasons.

One reason for this discrepancy might be the resolution of the model simulations. In previous studies a variety of resolutions were used (especially in the multi model approaches by Eyring et al. (2007) and Hoor et al. (2009). Our horizontal resolution of $\approx 2.8°$ is at the finer end of most of these resolutions (only Dalsøren et al. (2009) used $\approx 1.875°$). A coarse resolution leads to a strong dilution of the shipping emissions. This effect can lead to an overestimation of the O_3 production (e.g. Wild and Prather, 2006). Our results are also influenced by this problem too, because a resolution of T42 dilutes the emissions over large areas. A model with finer resolution, effective emissions, or a plume model (e.g. Franke et al., 2008; Holmes et al., 2014) diagnoses likely smaller contributions. Another important contributor to the differences is the geographical distribution of ship emissions. If the ship tracks are too narrow, the ozone production might be suppressed (see discussion by Eyring et al., 2007). Further, differences in the seasonal cycles of emissions con contribute to the differences.

4 Comparing perturbation and tagging approach

As discussed in the previous section and by previous studies (e.g. Wu et al., 2009; Grewe et al., 2010) the perturbation approach, which is often used for source attribution, and the tagging approach lead to different results.

To investigate this effect in more detail, the differences between the results of the *BASE* and *LTRA95* simulations with respect to O_3 are calculated

$$\Delta O_3 = {O_3}^{\mathrm{unperturbed}} - {O_3}^{\mathrm{perturbed}}, \tag{3}$$

where ${O_3}^{\mathrm{perturbed}}$ and ${O_3}^{\mathrm{unperturbed}}$ are the tropospheric O_3 columns from the simulation with 5 % reduced emissions and the original simulation, respectively. Similar $\Delta O_3^{\mathrm{tra}}$, the difference of the tagged ozone due land transport emissions, is calculated.

Atmos. Chem. Phys. Discuss., https://doi.org/10.5194/acp-2017-747
Manuscript under review for journal Atmos. Chem. Phys.
Discussion started: 12 October 2017

Atmospheric Chemistry and Physics Discussions

In a next step we calculate the ratios $\Delta O_3^{tra}/\Delta O_3$. This ratio indicates by how much the results using the tagging approach differ from the results of the perturbation approach.

The corresponding values of the partial columns up to 850 hPa are shown in Fig. 4. In general the ratio is largest in the Northern Hemisphere, where most land transport sources are located. In most regions the ratio is around 1.5–2. Over South America the ratio is one, so the tagging and the perturbation method show the same results, but in this region land transport emissions are rather small. Especially near the hotspot regions (Europe, Southeast Asia) ratios of up to 4 are simulated. Accordingly, the perturbation approach largely underestimates the contribution of land transport emissions to ozone in the regions of large land transport emissions.

To understand the reason for the different ratios in different regions in more detail, the dependency between NO_x emissions and the net O_3 production of the results for the year 2010 is analysed. Figure. 5a shows this dependency for the whole globe (black) and some chosen areas (coloured dots). Generally the the well known dependency (e.g. Seinfeld and Pandis, 2006) between O_3 production and NO_x concentrations can be observed. In pristine regions a net loss of O_3 is present (first regime). With increasing NO_x emissions the net O_3 production increases strongly. This second regime is usually called NO_x limited. The production of O_3 decrease again with even larger NO_x values. In this third regime, however, the production of O_3 can be increased if the $NMHC$ emissions are increased (called NMHC-limited). Every dot represents a different grid box of the model with different meteorological conditions and background mixing ratios of CO, NMHC etc. Therefore, the dependency between the NO_x mixing ratio and the net O_3 production differs for every grid box and is not given by one single function (which is the case for boxmodel calculations with prescribed conditions). In different regions of the world the O_3 production takes place in different chemical regimes, depending on the amount of NO_x emissions. Therefore, the coloured dots highlight the individual relationship between NO_x mixing ratio and production of O_3 for four different regions.

Depending on the regime of the O_3 production and the strength of the perturbation in the individual regions, the O_3 production responds differently on emissions in the different regions (e.g., Dahlmann et al., 2011). To illustrate this in more detail, the dots in Fig. 5b show the average dependency between NO_x and net O_3 production for the different geographical regions. Additionally, we calculated the estimated derivative of the ozone sensitivity based on the perturbed and the unperturbed simulation (see Grewe et al., 2010, for a in depth discussion with idealised examples as well as Fig.5c). Based on the estimated derivatives a saturation indicator Γ can be calculated, which is defined as:

$$\Gamma = \frac{\mathrm{y-axis\ intercept}}{\mathrm{y-value\ of\ unperturbed\ simulation}}, \tag{4}$$

with y being the net O_3 production rate (cf. Fig. 5).

This value is a quantitative measure of how the ozone production in the different region responds to a change of the emission strength. $\Gamma = 0$ indicates a linear response of the system (with an y-intercept at zero). $\Gamma = 1$ indicates a saturated behaviour of the ozone production i.e. the ozone production does not change, if emissions are changed. This point corresponds to the threshold between the NO_x- and $NMHC$- limited regime. $\Gamma > 1$ indicates an overcompensation effect, i.e., reduced NO_x emissions lead to an increase of the ozone production (corresponding to the $NMHC$-limited regime).

Atmos. Chem. Phys. Discuss., https://doi.org/10.5194/acp-2017-747
Manuscript under review for journal Atmos. Chem. Phys.
Discussion started: 12 October 2017

Atmospheric Chemistry and Physics Discussions

Accordingly (see Fig. 5b), the response of the net ozone production on the emissions perturbation in North Africa ($\Gamma = 0.3$) and South America ($\Gamma = 0.4$) is almost linear. In South-East-Asia ($\Gamma = 0.6$) the ozone production response is between the linear and saturated behaviour, while over Europe the ozone production is almost saturated ($\Gamma = 0.9$).

This shows that a reduction of land transport emissions in Europe would only slightly alter the ozone budget, because the efficiency of ozone production from other emission sources increases, if land transport emissions are decreased (Grewe et al., 2012).

This example clearly shows the importance of the discrimination of the tagging and the perturbation approach. Clearly both approaches answer different, but equally important questions. The perturbation approach answers the question on the impact of an emission reduction. This approach is important to estimate effects due to mitigation measures (e.g. Williams et al., 2014). The tagging approach in contrast, disentangles the ozone budget into the contributions of the individual emission sectors and is important to investigate e.g. the contribution of radiative forcing of individual emission sources. However, even if mitigation options are investigated the Tagging approach should be combined with the perturbation approach (see next subsection).

4.1 Combining Tagging and Perturbation approach in mitigation studies

The response of the atmospheric composition on a change of emissions can not be obtained from only one simulation using the tagging approach. This requires an additional simulation with changed emissions (perturbation approach), but the perturbed and the unperturbed simulation should be both equipped with a tagging diagnostic. In this case, the tagging diagnostics allows to quantify the contribution of the emissions from the sector of interest. Usually, the reduction of the contribution is much larger than the reduction of ozone itself, because the efficiency of the ozone productivity from the other sectors can be altered, even if the emissions themselves are unchanged. Combining the tagging and the perturbation approach is therefore the best way to measure the success of a mitigation strategy. If only the perturbation approach is used to evaluate a mitigation strategy, the success of one specific mitigation option largely depends on the history of previous mitigations (Grewe et al., 2012). This problem is sketched in Fig. 6. For each of the idealised mitigation options we assume a decrease of the emissions by 10 arbitrary units. Mitigation option 1 reduces the land transport emissions, mitigation option 2 the shipping emissions and mitigation option 3 the emissions from industry. If the resulting ozone concentration is considered (Fig. 6a) only mitigation option 3 seems to be successful. Due to mitigation option 1, however, the contribution of land transport emissions to the ozone concentration decreases, but the ozone production efficiency of all other emissions increases. Mitigation option 2 decreases the contribution of shipping emissions (which are reduced in this case), while the overall ozone concentration does not change. The large effect of the ozone concentration for option 3 is only the effect of all previous mitigation options. In contrast, if the emissions from industry instead of the land transport emissions are reduced in mitigation option 1, this mitigation would almost have no effect on the ozone concentration. This demonstrates the importance of combining perturbation and tagging to evaluate mitigation options.

Atmos. Chem. Phys. Discuss., https://doi.org/10.5194/acp-2017-747
Manuscript under review for journal Atmos. Chem. Phys.
Discussion started: 12 October 2017

Atmospheric Chemistry and Physics Discussions

5 Analysis of the ozone budget

For more details about the influence of emissions of land transport and ship traffic on the ozone burden, we analysed the burden as well as production and loss rates of O_3, O_3^{tra} and O_3^{shp}, respectively. These analyses were performed globally, as well as for the distinct geographical regions defined in Sect. 2.

The global total tropospheric burden of O_3 averaged for 2006–2010 is 318 Tg, which is in the range of 337 ± 23 Tg presented by Young et al. (2013), but please note that we used a fixed value of 200 hPa for the tropopause. Of these 318 Tg, globally 24 Tg are produced by land transport emissions, while 18 Tg are produced by emissions from shipping. The relative contribution of the burden of O_3^{tra} to the total ozone is thus around 8 % globally and 10 % in the regions Europe, North America and Southeastern Asia. The relative contribution of the burden of O_3^{shp} is around 6 % globally and 8 % near the important source regions. The difference between the rather large contribution of the shipping emissions near ground level (cf. Sect. 3) and the much smaller contribution for the whole troposphere is mainly caused by the confinement of the contribution of shipping emissions to the lowermost troposphere (e.g. Eyring et al., 2007; Hoor et al., 2009).

To better understand the effect of land transport and shipping emissions on the atmospheric composition, we analysed the production and loss rates of O_3 from land transport and shipping emissions globally and for the individual regions, respectively. The corresponding numbers are shown in Figs. 7 and 8. Globally integrated production rates of 5274 Tg a^{-1} (averaged 2006–2010) are simulated, while the loss rate is 3972 Tg a^{-1}, leading to a net production of O_3 of 1301 Tg a^{-1}. Similar values of 5110 ± 606 Tg a^{-1} for the production are reported by Young et al. (2013). The values of the loss are lower than reported by Young et al. (2013), but still within the spread of the different models (4668 ± 727 Tg a^{-1}, again note different definition of the tropopause). Globally a net production of 165 Tg a^{-1} from the land transport category is simulated, corresponding to a contribution of 13 % to the total net O_3 production. The contribution of the land transport category to the total net O_3 production near the source regions is 19 % over Europe (24 Tg a^{-1}), 21 % over North America (39 Tg a^{-1}) and 17 % over Southeast Asia (51 Tg a^{-1}).

A global net O_3 production of emissions from shipping of 129 Tg a^{-1} is simulated, corresponding to a contribution of 10 % to the total net O_3 production. Regionally, the importance of the shipping category to the net O_3 production is much larger. Here contributions of 34 % over the Northern Atlantic (26 Tg a^{-1}), 19 % over the Indian Ocean (17 Tg a^{-1}) and 52 % over the Northern Pacific (36 Tg a^{-1}) are simulated. The larger relative contributions near the source regions compared to the land transport category are mainly caused by less or almost no emissions of other sources in the shipping region. Especially over land, other important sources, such as anthropogenic non traffic and NO_x emissions from soil, decrease the relative importance of the land transport emissions. However, even near the source regions emissions of land transport contribute to around 20 % to the net O_3 production in these regions.

Atmos. Chem. Phys. Discuss., https://doi.org/10.5194/acp-2017-747
Manuscript under review for journal Atmos. Chem. Phys.
Discussion started: 12 October 2017

Atmospheric Chemistry and Physics Discussions

6 Radiative Forcing

We performed additional simulations to calculate the stratosphere adjusted radiative forcing (RF, e.g. Hansen et al., 1997; Stuber et al., 2001; Dietmüller et al., 2016) of land transport and ship traffic contributions to O_3. In these simulations only the dynamical processes and the radiation calculation are considered.

The monthly mean fields of the simulation *RC1SD-base-10a* are used as input data for the radiation scheme. To determine the contribution of the land transport and the ship emissions of the tagging results, the monthly means of 'O_3 minus O_3^{tra}' and 'O_3 minus O_3^{shp}' were fed into additional radiative calculation calls (Dietmüller et al., 2016). Finally, we calculated the stratospheric adjusted radiative forcing of O_3^{tra} and O_3^{shp} by subtracting the fluxes of 'O_3 minus O_3^{tra}' (analogue for O_3^{shp}) from the fluxes of O_3 (see also Dahlmann et al., 2011). The approach to calculate the RF by the results of the perturbation approach is similar to e.g. Myhre et al. (2011). We first calculate ΔO_3 between the unperturbed and the perturbed simulation and multiply this difference with a factor of 20. This scaled difference is then treated exactly as O_3^{tra} and O_3^{shp} to calculate the RF. In general we consider only the direct RF due to changes of the O_3 concentration. We calculate no RF due to changes of the methane concentration caused by the anthropogenic emissions. These changes would lead to a negative RF due to decreased methane concentrations. Especially for shipping emissions the negative RF due to methane can be larger compared to the positive ozone forcing (e.g. Myhre et al., 2011).

We obtain a global net RF for land transport of 92 $\mathrm{mW\ m^{-2}}$. The shortwave RF is 32 $\mathrm{mW\ m^{-2}}$ and the longwave RF is 61 $\mathrm{mW\ m^{-2}}$. The RF of ship traffic is 62 $\mathrm{mW\ m^{-2}}$ and smaller than the land transport RF. The shortwave RF of ship emissions is 22 $\mathrm{mW\ m^{-2}}$ and the longwave is 40 $\mathrm{mW\ m^{-2}}$. To review estimates of the RF of land transport and shipping emissions and to compare our results with previous estimates, Table 7 compares our results with previous studies. As noted above only the RF of O_3 is shown, RF of changed due to CH_4 are not considered.

Most studies have estimated a lower RF of land transport/road traffic emissions of around 30 $\mathrm{mW\ m^{-2}}$. These studies use the perturbation approach. Only Dahlmann et al. (2011) give larger estimates of around 170 $\mathrm{mW\ m^{-2}}$. They, however, used global land transport NO_x emissions of roughly 13 $\mathrm{Tg(N)\ a^{-1}}$ and a tagging method which considers NO_x only. Comparing the RF per $\mathrm{Tg(N)\ a^{-1}}$ Dahlmann et al. (2011) reported values of around 14 $\mathrm{mW\ m^{-2}\ Tg^{-1}(N)\ a}$, while our estimates are around 10 $\mathrm{mW\ m^{-2}\ Tg^{-1}(N)\ a}$.

Also for the RF due to shipping emissions previous estimates using the perturbation method (around 20–30 $\mathrm{mW\ m^{-2}}$) are lower compared to our findings of around 60 $\mathrm{mW\ m^{-2}}$. Only the tagging study by Dahlmann et al. (2011) report values which are more similar to our estimates (49 $\mathrm{mW\ m^{-2}}$), but this study used lower ship emissions of around 4 $\mathrm{Tg(N)\ a^{-1}}$ while we applied roughly 6 $\mathrm{Tg(N)\ a^{-1}}$. Accordingly, our results suggest an RF of 10 $\mathrm{mW\ m^{-2}\ Tg^{-1}(N)\ a}$, while Dahlmann et al. (2011) reported values of around 12 $\mathrm{mW\ m^{-2}\ Tg^{-1}(N)\ a}$.

For a more detailed comparison we also calculated the RF due to land transport and shipping using the 5 % perturbation method. By this method we estimate a global net RF of around 24 $\mathrm{mW\ m^{-2}}$ (scaled to 100 %) for land transport emissions and around 22 $\mathrm{mW\ m^{-2}}$ (scaled to 100 %) for shipping emissions. Both values are at the lower end of previous estimates of the RF using the perturbation approach. Remarkable, however, is the difference of a factor of three to four between our results using

Atmos. Chem. Phys. Discuss., https://doi.org/10.5194/acp-2017-747
Manuscript under review for journal Atmos. Chem. Phys.
Discussion started: 12 October 2017

the perturbation and the tagging approach, despite identical model and emissions. Accordingly, especially for calculations of radiative forcings, it is very important to differentiate between the tagging and the perturbation approach and the different scientific questions they answer.

The zonal averages of the shortwave, longwave and net radiative forcing for land transport and ship traffic are shown in Fig. 9. Solid (dashed) lines indicate the RF due to the tagging (perturbation) method. The overall behaviour of RFs deduced by tagging and perturbation method compare very well. However, the RF obtained by the tagging method is much larger than the RF obtained by the perturbation method. In particular, the peak at around 20°N is more enhanced for the tagging method. This is caused by the fact that the tagging method leads to larger O_3^{tra} values in the upper troposphere compared to the perturbation approach. Especially in this area O_3 is most radiative active. In all cases, the longwave radiative forcing with ≈ 65 % dominates over the shortwave radiative forcing with ≈ 35 %. The overall shape of the net forcing corresponds to the tropospheric O_3^{tra} and O_3^{shp} column (not shown). In general, the RFs of land transport and ship traffic are largest in the Northern Hemisphere, where most emissions occur. The overall behaviour of the RF zonal means compares quite well with that reported by Myhre et al. (2011), however, we simulate larger absolute values as discussed above.

Figure 10 shows the vertical profile of land transport and ship traffic radiative forcing for the tagging and perturbation method. Tagging and perturbation method show the same behaviour. However, the tagging method has larger values. Most flux changes are simulated in the lower/middle troposphere (300–1000 hPa). Here, the shortwave RF is negative. In contrast, the longwave forcing is positive throughout the whole atmosphere. The vertical profiles correspond to the fraction of O_3^{tra} (respectively O_3^{shp}) to O_3: the fraction increases with height until it peaks at 850 hPa. In this regime, the largest flux changes occur as well. Above, it continuously decreases with height, so do the flux changes.

7 Uncertainties

The general limitations of the tagging diagnostics applied in this study have been discussed by Grewe et al. (2017), therefore we here discuss only the most important details. The mathematical method itself is accurate, but the implementation into the model requires some simplifications like the introduction of chemical families. Recent updates of the tagging scheme with respect to differences of the HO_x family show an influence of some percent on the values of O_3 (Rieger et al 2017, in prep.). Therefore the error trough these simplifications is estimated to be smaller than the errors due to model simplifications and assumptions (physics and or chemistry, e.g. 20 % given by Eyring et al., 2007). For the future it would be very interesting to compare results from different tagging methods in more detail to have more quantitative information about the influence of the simplifications chosen by different methods. To our knowledge, however, no other tagging schemes with similar complexity as the scheme applied by us exist so far.

Clearly, the largest source of uncertainties are the emission inventories. Especially for source attribution not only the uncertainties of the emissions source of interest are important, but also the uncertainties of all other emissions sources. As an example, the emissions of NO_x from soil are poorly constrained (e.g. Vinken et al., 2014). This is in particular problematic

Atmos. Chem. Phys. Discuss., https://doi.org/10.5194/acp-2017-747
Manuscript under review for journal Atmos. Chem. Phys.
Discussion started: 12 October 2017

as part of the soil-NO_x emissions take place in similar regions as the land transport emissions. Therefore NO_x from both emissions sources influences the ozone production concurrently.

8 Summary and Conclusion

We estimate the contribution of land transport and shipping emissions to tropospheric ozone for the first time with an advanced tagging method which considers not only NO_x, but also CO and $NMHC$.

Our results indicate a maximum contribution of land transport emissions during summer of up to 18 % to ground level ozone in North America and 16 % in Southern Europe, which corresponds to up to 12 $\mathrm{nmol\ mol^{-1}}$ in North America and 10 $\mathrm{nmol\ mol^{-1}}$ in Europe.

The largest contribution of shipping emissions to ground level ozone was simulated in the Northern Pacific and the Northern Atlantic. During summer, contributions of up to 30 % were simulated in the Northwestern Pacific, corresponding to up to 12 $\mathrm{nmol\ mol^{-1}}$. In the Northern Atlantic contributions of up to 20 % during summer were calculated (up to 12 $\mathrm{nmol\ mol^{-1}}$). The comparison with previous estimates clearly show that the results strongly depend on the chosen method. Perturbation studies using a 5 % approach usually show the lowest contribution (scaled to 100 %) in the regions considered, while most 100 % perturbations, as well as the tagging approach show the largest contributions.

Overall, emissions of land transport and ship traffic contribute by 8 % and 6 %, respectively, to the tropospheric ozone burden. Land transport emissions contribute by around 20 % to the tropospheric ozone production near the source regions. The contribution of shipping emissions to the net ozone production near the source regions is with values of up to 52 % in the Northern Pacific even larger as the contribution of land transport emissions to the net production.

We estimate a global average radiative forcing due to ozone caused by land transport emissions of 92 $\mathrm{mW\ m^{-2}}$ and 62 $\mathrm{mW\ m^{-2}}$ caused by to ship emissions. In general, radiative forcings are largest on the Northern Hemisphere and peak at around 30° N. While our estimates of the contribution of land transport/shipping emissions to tropospheric ozone are similar compared to previous studies using a 100 % perturbation, our estimates of the radiative forcing are larger by a factor of 2–3 compared to previous estimates using the perturbation method.

Our results clearly show that a differentiation between results using the tagging and the perturbation method is very important. This holds especially for investigations of the radiative forcing, because both approaches give answers to different questions. The perturbation approach measures the effect of an emission reduction (or increase), while only the tagging approach yields contributions of individual emission sources to ozone concentration. This difference is very important when interpreting the results, in particular when investigating the radiative forcing of individual emission categories. To investigate mitigation options, the tagging method cannot replace sensitivity studies and vice versa. However, we clearly demonstrated that a combination of both methods strengthen the investigation of mitigation options and should be the method of choice.

Atmos. Chem. Phys. Discuss., https://doi.org/10.5194/acp-2017-747
Manuscript under review for journal Atmos. Chem. Phys.
Discussion started: 12 October 2017

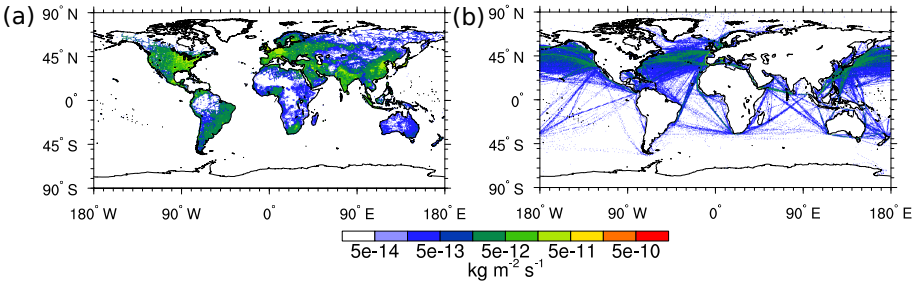

Figure 1. Average (2006–2010) emissions flux of NO_x (in $kg(N)\ m^{-2}\ s^{-1}$) emissions from **(a)** land transport and **(b)** shipping.

Table 1. Description of the different categories as used by the TAGGING submodel.

tagging categories	description
land transport	emissions of road traffic, inland navigation, railways (IPCC code 1A3b_c_e)
anthropogenic non-traffic	sectors Energy, Solvents, Waste, Industries, Residential, Agriculture
ship	emissions from ships (IPCC code 1A3d)
aviation	emissions from aircraft
lightning	lightning NO_x emissions
biogenic	on-line calculated isoprene and soil-NO_x emissions, off-line emissions from biogenic sources and agricultural waste burning (IPCC code 4F)
biomass burning	biomass burning emissions
CH_4	degradation of CH_4
N_2O	degradation of N_2O
stratosphere	downward transport from the stratosphere

Atmos. Chem. Phys. Discuss., https://doi.org/10.5194/acp-2017-747
Manuscript under review for journal Atmos. Chem. Phys.
Discussion started: 12 October 2017

Atmospheric Chemistry and Physics Discussions

Table 2. Average (2006–2010) annual total emission of CO (in $\mathrm{Tg(CO)\ a^{-1}}$), $\mathrm{NO_x}$ (in $\mathrm{Tg(N)\ a^{-1}}$) and NMHC (in amount of carbon) of the most important emission categories. The category 'other' contains the emissions of the sectors biomass burning, agricultural waste burning as well as other biogenic emissions.

	CO ($\mathrm{Tg(CO)\ a^{-1}}$)	NMHC ($\mathrm{Tg(C)\ a^{-1}}$)	$\mathrm{NO_x}$ ($\mathrm{Tg(N)\ a^{-1}}$)
land transport	152	17	10
shipping	1	2	6
anthropogenic non-traffic	411	73	17
soil NOx			6
lightning NOx			5
biogenic $\mathrm{C_5H_8}$		493	
other	416	15	5

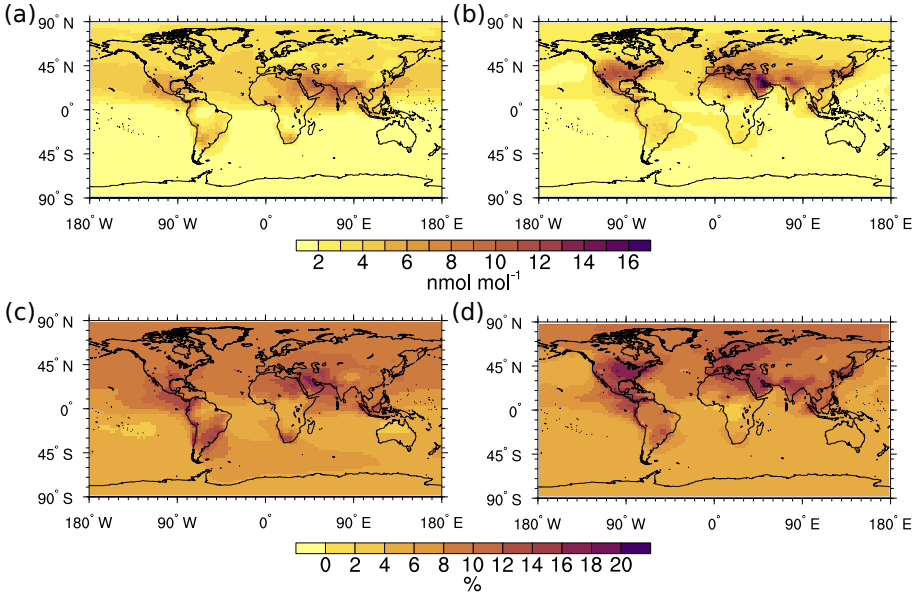

Figure 2. Seasonal average values of the absolute and relative contribution of $\mathrm{O_3^{tra}}$ to near ground level $\mathrm{O_3}$. The upper row give the absolute values (in $\mathrm{nmol\ mol^{-1}}$ for winter (DJF, **(a)**) and summer (JJA, **(b)**), respectively. The lower row shows the DJF **(c)** and JJA **(d)** values of the contribution (in %).

Atmos. Chem. Phys. Discuss., https://doi.org/10.5194/acp-2017-747
Manuscript under review for journal Atmos. Chem. Phys.
Discussion started: 12 October 2017

Atmospheric Chemistry and Physics Discussions

Table 3. Summary of previous global model studies investigating the contribution/impact of land transport/road traffic emissions to ozone. Method denotes the percentage of the emissions reductions (perturbation). The other columns list the amount of land transport/road traffic emissions as well as the fraction (f) compared to the emissions used in the studies for NO_x (in $Tg(N)\ a^{-1}$), CO (in $Tg(CO)\ a^{-1}$) and NMHC ($Tg(C)\ a^{-1}$). The four rows from the right list the contribution of the land transport/road traffic categories as estimated by these studies in mixing ratios and/or percent. Where possible, we show the estimated contribution for the geographical regions defined in Sect. 2 as well as zonal average values. All contributions are given to near ground level ozone and for July conditions. The table is ordered by the year of publication. A '-' indicates missing information.

study	method	NO_x	fNO_x	CO	fCO	NMHC	fNMHC	NA	EU	SEA	ZM
								$nmol\ mol^{-1}$	$nmol\ mol^{-1}$	$nmol\ mol^{-1}$	$nmol\ mol^{-1}$
		$Tg\ a^{-1}$	%	$Tg\ a^{-1}$	%	$Tg\ a^{-1}$	%	%	%	%	%
GB03	100%	10	24	207	14	-	-	-	-	-	-
								11–15	9–15	5–12	-
NM06	100%	9	30[a]	196	36[a]	36	27[a]	5–20	5–15	5–10	-
								10–50	-5–25	5–50	-
NM06	100%	9	30[a]	196	36[a]	36	27[a]	zonal mean			-
											up to 10
M07	100%	9	24	237	-	27	5	-	-	-	-
								13–16	9–16	3–16	-
M07	100%	9	24	237	-	27	5	zonal mean			up to 5
											up to 12
H09	5 %[b]	7	15	31	7	8	2	2–5[c]	2–6[c]	1–4[c]	-
								-	-	-	-
K10	5 %[b]	9	18	110	11	11	1	2–5	-1–5	1–3	-
								-	-	-	-
K10	100 %	9	18	110	11	11	1	zonal mean ground level			-
											up to 7
this study	tagging	10	20	152	16	17	3	3–14	3–13	2–11	
								6–19	8–18	5–16	
this study	tagging	10	20	152	16	17	3	zonal mean mid latitudes NH			3–7
											9–11
this study	5 %[b]	10	20	152	16	17	3	1–9	-1–6	-1–5	-
								1–12	-3–9	-2–12	-
this study	5 %[b]	10	20	152	16	17	3	zonal mean mid latitudes NH			2–4
											1–2

[a] Fraction only compared to all anthropogenic emissions. [b] Given values scaled to 100 %. [c] Given for average values from 800 hPa to the surface.
Abbreviations are: GB03 (Granier and Brasseur, 2003), N06 (Niemeier et al., 2006), M07 (Matthes et al., 2007), H09 (Hoor et al., 2009), K10 (Koffi et al., 2010).

Atmos. Chem. Phys. Discuss., https://doi.org/10.5194/acp-2017-747
Manuscript under review for journal Atmos. Chem. Phys.
Discussion started: 12 October 2017

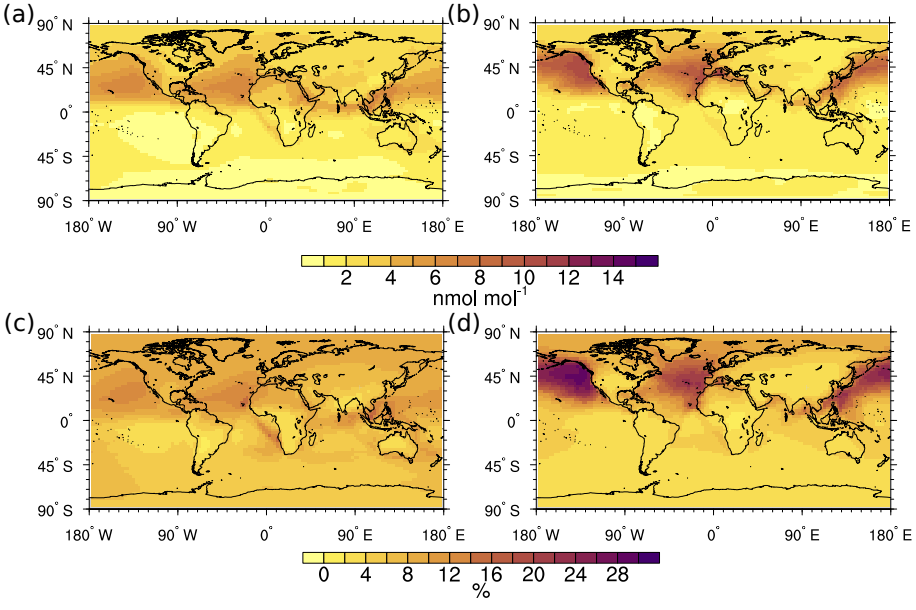

Figure 3. Seasonal average values of the absolute and relative contribution of O_3^{shp} to near ground level O_3. The upper row give the absolute values (in $nmol\ mol^{-1}$ for DJF **(a)** and JJA **(b)**, respectively. The lower row shows the DJF **(c)** and JJA **(d)** values of the contribution (in %).

Atmos. Chem. Phys. Discuss., https://doi.org/10.5194/acp-2017-747
Manuscript under review for journal Atmos. Chem. Phys.
Discussion started: 12 October 2017

Atmospheric Chemistry and Physics Discussions

Table 4. Summary of previous global model studies investigating the contribution/impact of shipping emissions to ozone. Method denotes the percentage of the emissions reductions (perturbation). The other columns list the amount of shipping emissions as well as the fraction (f) compared to all emissions used in the studies for NO_x (in $Tg(N)\ a^{-1}$). The four rows from the right list the contribution of the shipping category as estimated by these studies in mixing ratios (upper row) and/or percent (lower row). Where possible, we show the estimated contribution for the geographical regions defined in Sect. 2 as well as zonal average values. For the geographical regions we give only the values larger than the background values. All contributions are given to near ground level ozone and for July conditions. The table is ordered by the year of publication. A '-' indicates missing information.

study	method	NO_x	fNO_x	Atlantic	Pacific	India	Zonal Mean
				$nmol\ mol^{-1}$	$nmol\ mol^{-1}$	$nmol\ mol^{-1}$	$nmol\ mol^{-1}$
		$Tg\ a^{-1}$	%	%	%	%	%
ED03	100%	4	8	4–12	4–11	3–4	-
				-	-	-	-
E07	100%	3	11[a]	2–12	1–4	1–4	-
				12–36	12–24	12–18	-
E07	100%	3	11[a]	zonal mean mid latitude NH			1–1.5
							-
H09	5%[c]	4	10	2–4	2–3	1–2	-
				-	-	-	-
D09	100 %	5	-	-	-	-	-
				14–33	14–40	9–12	-
K10	5%[c]	4	8	2–5	3–6	1–2	-
				-	-	-	-
K10	5%[c]	4	8	zonal mean			up to 1.5
							-
K10	100%	4	8	up to 8	up to 9	-	-
				-	-	-	-
K10	100%	4	8	zonal mean			up to 3
							-
this study	tagging	6	12	3–9	4–11	2–5	-
				10–24	10–33	9–15	-
this study	tagging	6	12	zonal mean mid latitudes NH			3–6
							10–15
this study	5 %[c]	6	12	2–8	2–7	1–4	-
				10–18	11–22	4–10	-
this study	5 %[c]	6	12	zonal mean mid latitudes NH			2–4
							5–8

[a] No information available. [b] Fraction only compared to all anthropogenic emissions. [c] Given values scaled to 100 %. [d] Given for average values from 800 hPa to the surface. Abbreviations are: ED03 (Endresen et al., 2003), E07 (Eyring et al., 2007), H09 (Hoor et al., 2009),D09 (Dalsøren et al., 2009), K10 (Koffi et al., 2010).

Atmos. Chem. Phys. Discuss., https://doi.org/10.5194/acp-2017-747
Manuscript under review for journal Atmos. Chem. Phys.
Discussion started: 12 October 2017

Atmospheric Chemistry and Physics Discussions

Table 5. Burden of O_3 and O_3^{tra} integrated up to 200 hPa (in Tg). Average values for the period 2006–2010.

	O_3 (Tg)	O_3^{tra} (Tg)	contribution O_3^{tra} (%)
Global	318	24	8
Europe	15	2	10
North America	21	2	10
Southeast Asia	25	2	9

Table 6. Burden of O_3 (total) and O_3^{shp} (shipping) integrated up to 200 hPa (in Tg). Average values for the period 2006–2010.

	O_3 (Tg)	O_3^{shp} (Tg)	contribution O_3^{shp} (%)
Global	318	18	6
North Atlantic Ocean	24	2	8
Indian Ocean	27	1	5
North Pacific Ocean	32	2	8

Atmos. Chem. Phys. Discuss., https://doi.org/10.5194/acp-2017-747
Manuscript under review for journal Atmos. Chem. Phys.
Discussion started: 12 October 2017

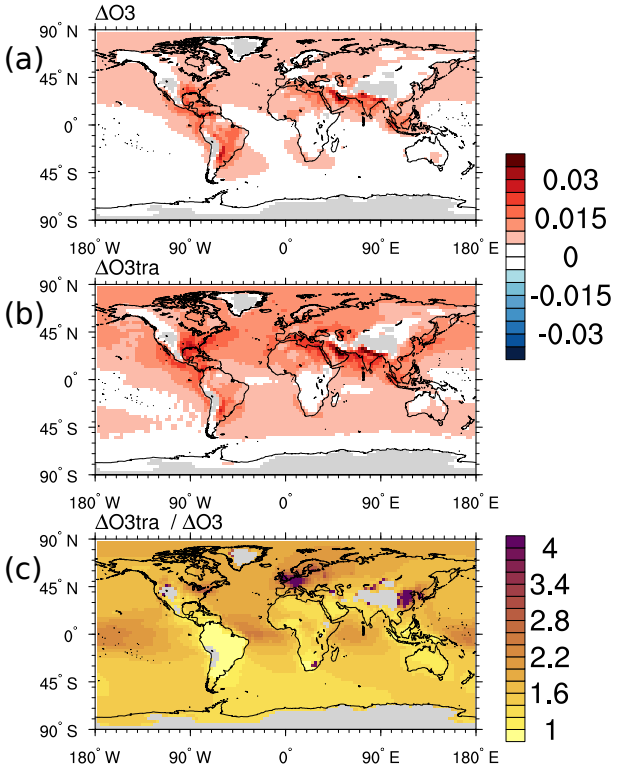

Figure 4. Multi-annual averages (2006–2010) of **(a)** ΔO_3, **(b)** $\Delta O_3^{tra}$and **(c)** $\Delta O_3^{tra}/\Delta O_3$. The differences are calculated for the partial columns from the surface of up to 850 hPa.

Atmos. Chem. Phys. Discuss., https://doi.org/10.5194/acp-2017-747
Manuscript under review for journal Atmos. Chem. Phys.
Discussion started: 12 October 2017

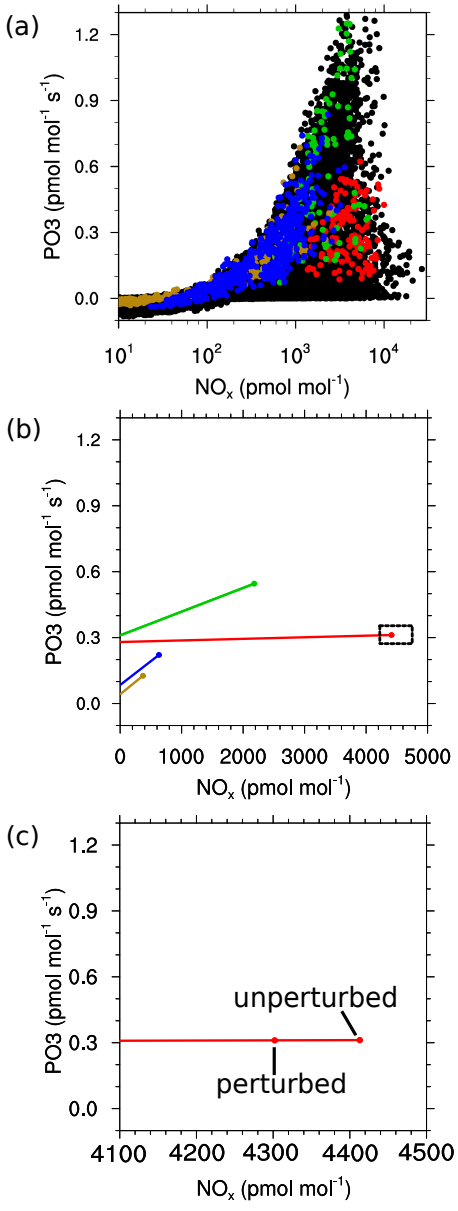

Figure 5. Dependency between NO_x mixing ratios and net O_3 production. (a) Gridbox values: The black dots represent monthly mean values at ground level for the year 2010 of every individual grid box. The individual colours indicate monthly average values during May–August (Northern Hemisphere) and November–February (Southern Hemisphere) for individual regions (defined as rectangular areas, see Appendix I). (b) Regional values: The single dots represent year 2010 averages for the four regions shown in (a). In addition the tangents were calculated for every region by comparing the perturbed and the unperturbed simulations. The black rectangle highlights the region shown in (c). The x-axes of (c) and (b) are linear, while (a) uses a logarithmic x-axis.

Atmos. Chem. Phys. Discuss., https://doi.org/10.5194/acp-2017-747
Manuscript under review for journal Atmos. Chem. Phys.
Discussion started: 12 October 2017

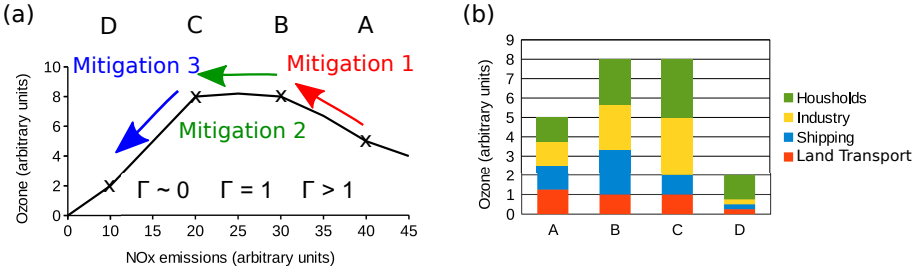

Figure 6. Idealised example explaining the difference of the perturbation and the tagging approach for the evaluation of mitigation increases. (a) shows the dependency between NO_x emissions and ozone (both in arbitrary units). Three different mitigation options are indicated by the colored arrows. In addition, the approximate value of Γ (see text for definition) is given. (b) shows the contribution of the ozone concentration at the four marked points in (a). In this example it is assumed that only four emission categories exist, emitting the same amount of emissions at point A.

Atmos. Chem. Phys. Discuss., https://doi.org/10.5194/acp-2017-747
Manuscript under review for journal Atmos. Chem. Phys.
Discussion started: 12 October 2017

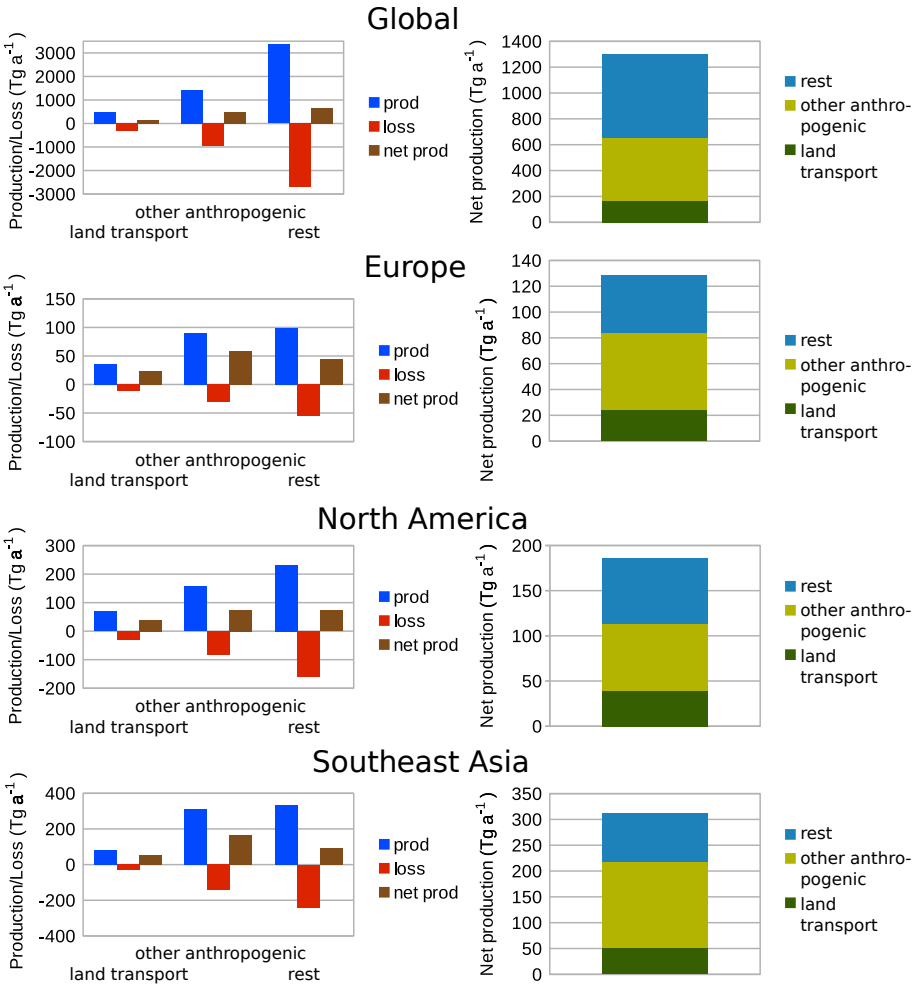

Figure 7. Production and loss rates of O_3 from different sectors (integrated up to 200 hPa and averaged for 2006–2010). The left side shows the individual production and loss rates as well as the net O_3 production, while the right side shows only the net production of the different sectors. For simplicity only land transport, other anthropogenic (shipping, anthropogenic non-traffic and aviation) and rest (all other tagging categories) are shown.

Atmos. Chem. Phys. Discuss., https://doi.org/10.5194/acp-2017-747
Manuscript under review for journal Atmos. Chem. Phys.
Discussion started: 12 October 2017

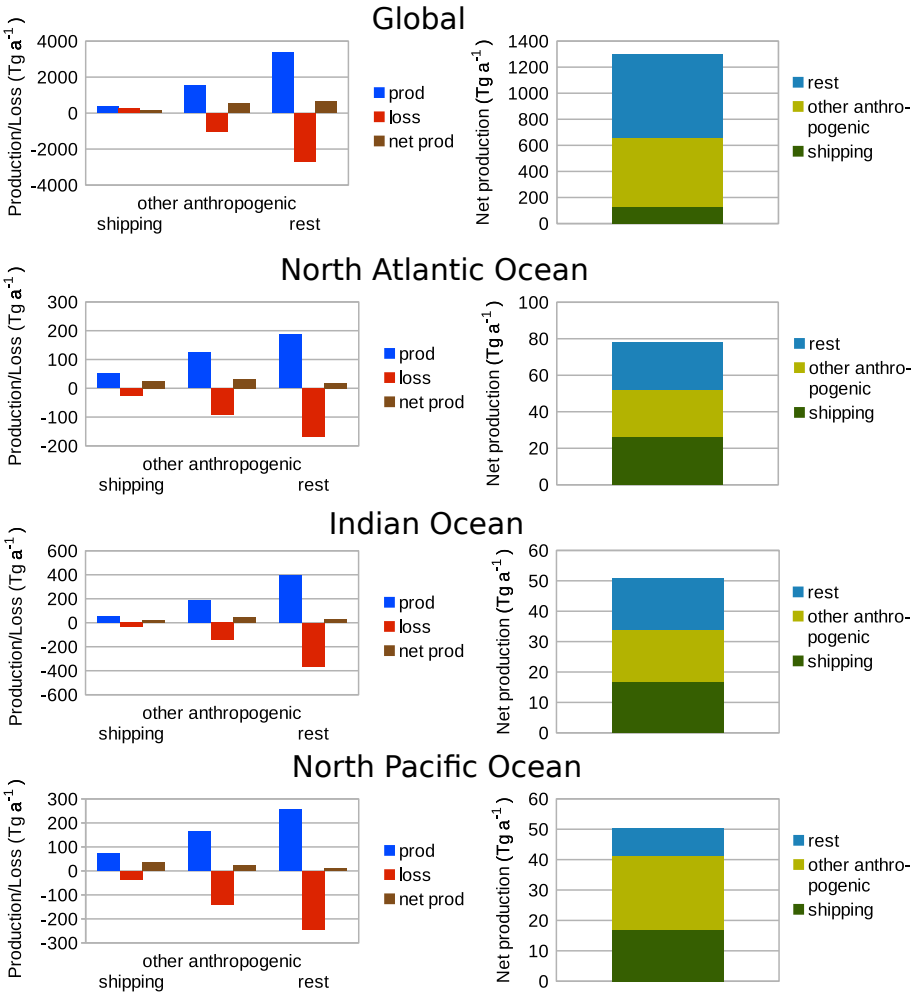

Figure 8. Production and loss rates of O_3 from different sectors (integrated up to 200 hPa and averaged for 2006–2010). The left side shows the individual production and loss rates as well as the net O_3 production, while the right side shows only the net production of the different sectors. For simplicity only shipping, other anthropogenic (land transport, anthropogenic non-traffic and aviation) and rest (all other tagging categories) are shown.

Atmos. Chem. Phys. Discuss., https://doi.org/10.5194/acp-2017-747
Manuscript under review for journal Atmos. Chem. Phys.
Discussion started: 12 October 2017

Atmospheric Chemistry and Physics Discussions

Table 7. Global estimates of the annually averaged radiative forcing due to O_3 caused by emissions of land transport/road traffic (global RF road) and ship emissions (global RF shp). Please note that individual studies use different methods for the calculation of the radiative forcing e.g. some studies give instantaneous values, while other studies stratospheric adjusted values (see last row).

Study	method	global RF road ($mW\ m^{-2}$)	global RF shp ($mW\ m^{-2}$)	RF type
Endresen et al. (2003)	100 %	-	29	scaling of tropospheric ozone column change
Niemeier et al. (2006)	100 %	30 / 50 (January / July)	-	instantaneous at TP[e]
Eyring et al. (2007)	100 %	-	10 ± 2	instantaneous at TP[e] decreased by 22 %
Fuglestvedt et al. (2008)	100 %	54 ± 11	32 ± 9	stratospheric adjusted
Hoor et al. (2009)	5 %	28[a]	28[a]	-
Dahlmann et al. (2011)[c]	tagging	170	49	fixed dynamical heating
Dahlmann et al. (2011)[c]	100 %	31	-	fixed dynamical heating
Myhre et al. (2011)	5 %	31[a]	24[a]	
Grewe et al. (2012)	tagging[c]	132	-	fixed dynamical heating
Grewe et al. (2012)	100 %[c]	24	-	fixed dynamical heating
Holmes et al. (2014)	5 %	-	27[d]	-
this study	tagging	92	62	stratospheric adjusted
this study	5 %	24[a]	22[a]	stratospheric adjusted

[a] Scaled to 100 %. [b] For year 2000 conditions. [c] For year 1990 conditions. [d]Calculated by scaling the RF value of the 'instant dilution' case for a change of 1 $Tg\ a^{-1}$ with the total amount of used emissions by Holmes et al. (2014). [e] Tropopause

Atmos. Chem. Phys. Discuss., https://doi.org/10.5194/acp-2017-747
Manuscript under review for journal Atmos. Chem. Phys.
Discussion started: 12 October 2017

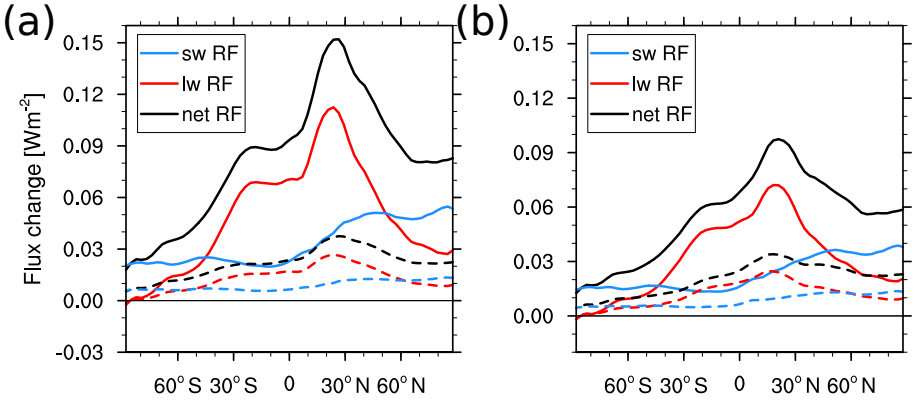

Figure 9. Zonal mean of shortwave, longwave and net radiative O_3 forcing of (a) land transport and (b) ship traffic. The continuous lines give the results of the tagging method, the dashed lines of the perturbation method.

Atmos. Chem. Phys. Discuss., https://doi.org/10.5194/acp-2017-747
Manuscript under review for journal Atmos. Chem. Phys.
Discussion started: 12 October 2017

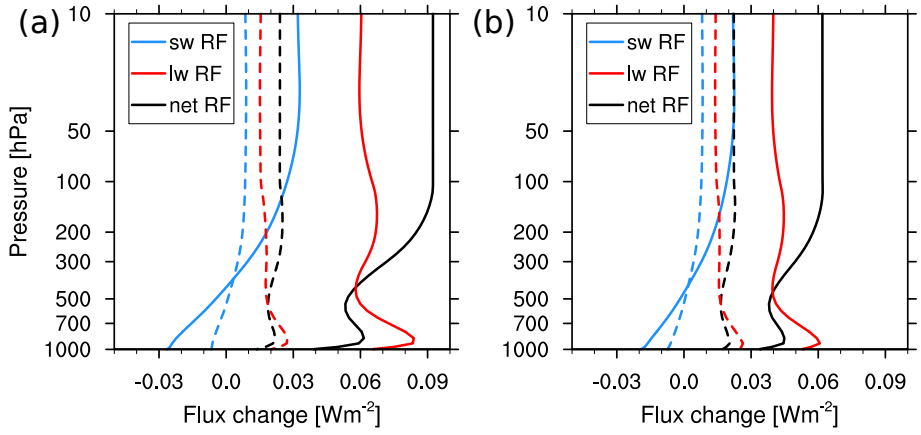

Figure 10. Vertical profile of globally averaged shortwave, longwave and net radiative O_3 forcing of (a) land transport and (b) ship traffic. The continuous lines give the results of the tagging method, the dashed lines of the perturbation method.

Atmos. Chem. Phys. Discuss., https://doi.org/10.5194/acp-2017-747
Manuscript under review for journal Atmos. Chem. Phys.
Discussion started: 12 October 2017

Acknowledgements. M.Mertens acknowledges funding by the DLR project 'Verkehr in Europa' and 'Auswirkungen von NO_x'. Furthermore part of this work is funded by the DLR internal project 'VEU2'. We thank R. Sausen and M. Righi (both DLR) for very helpful comments which improved this manuscript. Analysis and graphics of the used data was performed using the NCAR Command Language (Version 6.4.0) Software developed by UCAR/NCAR/CISL/TDD and available on-line: http://dx.doi.org/10.5065/D6WD3XH5. Computational resources for the simulation were provided by the German Climate Computing Centre (DKRZ) in Hamburg.

References

Butler, T., Lawrence, M., Taraborrelli, D., and Lelieveld, J.: Multi-day ozone production potential of volatile organic compounds calculated with a tagging approach, Atmospheric Environment, 45, 4082 – 4090, doi:http://doi.org/10.1016/j.atmosenv.2011.03.040, http://www.sciencedirect.com/science/article/pii/S1352231011003001, 2011.

Crutzen, Paul, J.: Photochemical reactions initiated by and influencing ozone in unpolluted tropospheric air, Tellus, 26, 47–57, doi:10.1111/j.2153-3490.1974.tb01951.x, http://dx.doi.org/10.1111/j.2153-3490.1974.tb01951.x, 1974.

Dahlmann, K., Grewe, V., Ponater, M., and Matthes, S.: Quantifying the contributions of individual NOx sources to the trend in ozone radiative forcing, Atmos. Environ., 45, 2860–2868, doi:http://dx.doi.org/10.1016/j.atmosenv.2011.02.071, http://www.sciencedirect.com/science/article/pii/S1352231011002366, 2011.

Dalsøren, S. B., Eide, M. S., Endresen, Ø., Mjelde, A., Gravir, G., and Isaksen, I. S. A.: Update on emissions and environmental impacts from the international fleet of ships: the contribution from major ship types and ports, Atmospheric Chemistry and Physics, 9, 2171–2194, doi:10.5194/acp-9-2171-2009, http://www.atmos-chem-phys.net/9/2171/2009/, 2009.

Deckert, R., Jöckel, P., Grewe, V., Gottschaldt, K.-D., and Hoor, P.: A quasi chemistry-transport model mode for EMAC, Geosci. Model Dev., 4, 195–206, doi:10.5194/gmd-4-195-2011, http://www.geosci-model-dev.net/4/195/2011/, 2011.

Dee, D. P., Uppala, S. M., Simmons, A. J., Berrisford, P., Poli, P., Kobayashi, S., Andrae, U., Balmaseda, M. A., Balsamo, G., Bauer, P., Bechtold, P., Beljaars, A. C. M., van de Berg, L., Bidlot, J., Bormann, N., Delsol, C., Dragani, R., Fuentes, M., Geer, A. J., Haimberger, L., Healy, S. B., Hersbach, H., Hólm, E. V., Isaksen, L., Kållberg, P., Köhler, M., Matricardi, M., McNally, A. P., Monge-Sanz, B. M., Morcrette, J.-J., Park, B.-K., Peubey, C., de Rosnay, P., Tavolato, C., Thépaut, J.-N., and Vitart, F.: The ERA-Interim reanalysis: configuration and performance of the data assimilation system, Quart. J. Roy. Meteor. Soc., 137, 553–597, doi:10.1002/qj.828, http://dx.doi.org/10.1002/qj.828, 2011.

Dietmüller, S., Jöckel, P., Tost, H., Kunze, M., Gellhorn, C., Brinkop, S., Frömming, C., Ponater, M., Steil, B., Lauer, A., and Hendricks, J.: A new radiation infrastructure for the Modular Earth Submodel System (MESSy, based on version 2.51), Geoscientific Model Development, 9, 2209–2222, doi:10.5194/gmd-9-2209-2016, http://www.geosci-model-dev.net/9/2209/2016/, 2016.

Emmons, L. K., Walters, S., Hess, P. G., Lamarque, J.-F., Pfister, G. G., Fillmore, D., Granier, C., Guenther, A., Kinnison, D., Laepple, T., Orlando, J., Tie, X., Tyndall, G., Wiedinmyer, C., Baughcum, S. L., and Kloster, S.: Description and evaluation of the Model for Ozone and Related chemical Tracers, version 4 (MOZART-4), Geosci. Model Dev., 3, 43–67, doi:10.5194/gmd-3-43-2010, http://www.geosci-model-dev.net/3/43/2010/, 2010.

Emmons, L. K., Hess, P. G., Lamarque, J.-F., and Pfister, G. G.: Tagged ozone mechanism for MOZART-4, CAM-chem and other chemical transport models, Geosci. Model Dev., 5, 1531–1542, doi:10.5194/gmd-5-1531-2012, http://www.geosci-model-dev.net/5/1531/2012/, 2012.

Endresen, Ø., Sørgård, E., Sundet, J. K., Dalsøren, S. B., Isaksen, I. S. A., Berglen, T. F., and Gravir, G.: Emission from international sea transportation and environmental impact, Journal of Geophysical Research: Atmospheres, 108, doi:10.1029/2002JD002898, http://dx.doi.org/10.1029/2002JD002898, 4560, 2003.

Eyring, V., Stevenson, D. S., Lauer, A., Dentener, F. J., Butler, T., Collins, W. J., Ellingsen, K., Gauss, M., Hauglustaine, D. A., Isaksen, I. S. A., Lawrence, M. G., Richter, A., Rodriguez, J. M., Sanderson, M., Strahan, S. E., Sudo, K., Szopa, S., van Noije, T. P. C., and Wild, O.: Multi-model simulations of the impact of international shipping on Atmospheric Chemistry and Climate in 2000 and 2030, Atmos. Chem. Phys., 7, 757–780, doi:10.5194/acp-7-757-2007, http://www.atmos-chem-phys.net/7/757/2007/, 2007.

Eyring, V., Isaksen, I. S., Berntsen, T., Collins, W. J., Corbett, J. J., Endresen, O., Grainger, R. G., Moldanova, J., Schlager, H., and Stevenson, D. S.: Transport impacts on atmosphere and climate: Shipping, Atmospheric Environment, 44, 4735 – 4771, doi:http://doi.org/10.1016/j.atmosenv.2009.04.059, http://www.sciencedirect.com/science/article/pii/S1352231009003379, transport Impacts on Atmosphere and Climate: The {ATTICA} Assessment Report, 2010.

Fowler, D., Pilegaard, K., Sutton, M., Ambus, P., Raivonen, M., Duyzer, J., Simpson, D., Fagerli, H., Fuzzi, S., Schjoerring, J., Granier, C., Neftel, A., Isaksen, I., Laj, P., Maione, M., Monks, P., Burkhardt, J., Daemmgen, U., Neirynck, J., Personne, E., Wichink-Kruit, R., Butterbach-Bahl, K., Flechard, C., Tuovinen, J., Coyle, M., Gerosa, G., Loubet, B., Altimir, N., Gruenhage, L., Ammann, C., Cieslik, S., Paoletti, E., Mikkelsen, T., Ro-Poulsen, H., Cellier, P., Cape, J., Horvàth, L., Loreto, F., Niinemets, U., Palmer, P., Rinne, J., Misztal, P., Nemitz, E., Nilsson, D., Pryor, S., Gallagher, M., Vesala, T., Skiba, U., Brüggemann, N., Zechmeister-Boltenstern, S., Williams, J., O'Dowd, C., Facchini, M., de Leeuw, G., Flossman, A., Chaumerliac, N., and Erisman, J.: Atmospheric composition change: Ecosystems-Atmosphere interactions, Atmospheric Environment, 43, 5193–5267, doi:http://dx.doi.org/10.1016/j.atmosenv.2009.07.068, http://www.sciencedirect.com/science/article/pii/S1352231009006633, ACCENT Synthesis, 2009.

Franke, K., Eyring, V., Sander, R., Hendricks, J., Lauer, A., and Sausen, R.: Toward effective emissions of ships in global models, Meteorologische Zeitschrift, 17, 117–129, doi:10.1127/0941-2948/2008/0277, http://dx.doi.org/10.1127/0941-2948/2008/0277, 2008.

Fuglestvedt, J., Berntsen, T., Myhre, G., Rypdal, K., and Skeie, R. B.: Climate forcing from the transport sectors, Proceedings of the National Academy of Sciences, 105, 454–458, doi:10.1073/pnas.0702958104, http://www.pnas.org/content/105/2/454.abstract, 2008.

Granier, C. and Brasseur, G. P.: The impact of road traffic on global tropospheric ozone, Geophys. Res. Lett., 30, doi:10.1029/2002GL015972, http://dx.doi.org/10.1029/2002GL015972, 2003.

Granier, C., Bessagnet, B., Bond, T., D'Angiola, A., van der Gon, H. D., Frost, G., Heil, A., Kaiser, J., Kinne, S., Klimont, Z., Kloster, S., Lamarque, J.-F., Liousse, C., Masui, T., Meleux, F., Mieville, A., Ohara, T., Raut, J.-C., Riahi, K., Schultz, M., Smith, S., Thompson, A., Aardenne, J., Werf, G., and Vuuren, D.: Evolution of anthropogenic and biomass burning emissions of air pollutants at global and regional scales during the 1980–2010 period, Clim. Change, 109, 163–190, 2011.

Grewe, V.: Technical Note: A diagnostic for ozone contributions of various NO_x emissions in multi-decadal chemistry-climate model simulations, Atmos. Chem. Phys., 4, 729–736, doi:10.5194/acp-4-729-2004, http://www.atmos-chem-phys.net/4/729/2004/, 2004.

Grewe, V.: A generalized tagging method, Geosci. Model Dev., 6, 247–4253, doi:10.5194/gmdd-5-3311-2012, http://www.geosci-model-dev-discuss.net/5/3311/2012/, 2013.

Grewe, V., Dameris, M., Fichter, C., and Sausen, R.: Impact of aircraft NOx emissions. Part 1: Interactively coupled climate-chemistry simulations and sensitivities to climate-chemistry feedback, lightning and model resolution, Meteorologische Zeitschrift, 11, 177–186, doi:10.1127/0941-2948/2002/0011-0177, http://dx.doi.org/10.1127/0941-2948/2002/0011-0177, 2002.

Grewe, V., Tsati, E., and Hoor, P.: On the attribution of contributions of atmospheric trace gases to emissions in atmospheric model applications, Geosci. Model Dev., 3, 487–499, doi:10.5194/gmd-3-487-2010, http://www.geosci-model-dev.net/3/487/2010/, 2010.

Grewe, V., Dahlmann, K., Matthes, S., and Steinbrecht, W.: Attributing ozone to NOx emissions: Implications for climate mitigation measures, Atmos. Environ., 59, 102–107, doi:10.1016/j.atmosenv.2012.05.002, http://www.sciencedirect.com/science/article/pii/S1352231012004335, 2012.

Grewe, V., Tsati, E., Mertens, M., Frömming, C., and Jöckel, P.: Contribution of emissions to concentrations: the TAGGING 1.0 submodel based on the Modular Earth Submodel System (MESSy 2.52), Geoscientific Model Development, 10, 2615–2633, doi:10.5194/gmd-10-2615-2017, https://www.geosci-model-dev.net/10/2615/2017/, 2017.

Guenther, A., Hewitt, C., E., D., Fall, R. G., C., Graedel, T., Harley, P., Klinger, L., Lerdau, M., McKay, W., Pierce, T., S., B., Steinbrecher, R., Tallamraju, R., Taylor, J., and Zimmermann, P.: A global model of natural volatile organic compound emissions, J. Geophys. Res., 100, 8873–8892, 1995.

Haagen-Smit, A. J.: Chemistry and Physiology of Los Angeles Smog, Industrial & Engineering Chemistry, 44, 1342–1346, doi:10.1021/ie50510a045, http://dx.doi.org/10.1021/ie50510a045, 1952.

Hansen, J., Sato, M., and Ruedy, R.: Radiative forcing and climate response, Journal of Geophysical Research: Atmospheres, 102, 6831–6864, doi:10.1029/96JD03436, http://dx.doi.org/10.1029/96JD03436, 1997.

Hendricks, J., Righi, M., Dahlmann, K., Gottschaldt, K.-D., Grewe, V., Ponater, M., Sausen, R., Heinrichs, D., Winkler, C., Wolfermann, A., Kampffmeyer, T., Friedrich, R., Klötzke, M., and Kugler, U.: Quantifying the climate impact of emissions from land-based transport in Germany, Transportation Research Part D: Transport and Environment, doi:https://doi.org/10.1016/j.trd.2017.06.003, 2017.

Holmes, C. D., Prather, M. J., and Vinken, G. C. M.: The climate impact of ship NO_x emissions: an improved estimate accounting for plume chemistry, Atmospheric Chemistry and Physics, 14, 6801–6812, doi:10.5194/acp-14-6801-2014, http://www.atmos-chem-phys.net/14/6801/2014/, 2014.

Hoor, P., Borken-Kleefeld, J., Caro, D., Dessens, O., Endresen, O., Gauss, M., Grewe, V., Hauglustaine, D., Isaksen, I. S. A., Jöckel, P., Lelieveld, J., Myhre, G., Meijer, E., Olivie, D., Prather, M., Schnadt Poberaj, C., Shine, K. P., Staehelin, J., Tang, Q., van Aardenne, J., van Velthoven, P., and Sausen, R.: The impact of traffic emissions on atmospheric ozone and OH: results from QUANTIFY, Atmos. Chem. Phys., 9, 3113–3136, doi:10.5194/acp-9-3113-2009, http://www.atmos-chem-phys.net/9/3113/2009/, 2009.

Jöckel, P., Tost, H., Pozzer, A., Brühl, C., Buchholz, J., Ganzeveld, L., Hoor, P., Kerkweg, A., Lawrence, M., Sander, R., Steil, B., Stiller, G., Tanarhte, M., Taraborrelli, D., van Aardenne, J., and Lelieveld, J.: The atmospheric chemistry general circulation model ECHAM5/MESSy1: consistent simulation of ozone from the surface to the mesosphere, Atmos. Chem. Phys., 6, 5067–5104, doi:10.5194/acp-6-5067-2006, http://www.atmos-chem-phys.net/6/5067/2006/, 2006.

Jöckel, P., Kerkweg, A., Pozzer, A., Sander, R., Tost, H., Riede, H., Baumgaertner, A., Gromov, S., and Kern, B.: Development cycle 2 of the Modular Earth Submodel System (MESSy2), Geosci. Model Dev., 3, 717–752, doi:10.5194/gmd-3-717-2010, http://www.geosci-model-dev.net/3/717/2010/, 2010.

Jöckel, P., Tost, H., Pozzer, A., Kunze, M., Kirner, O., Brenninkmeijer, C. A. M., Brinkop, S., Cai, D. S., Dyroff, C., Eckstein, J., Frank, F., Garny, H., Gottschaldt, K.-D., Graf, P., Grewe, V., Kerkweg, A., Kern, B., Matthes, S., Mertens, M., Meul, S., Neumaier, M., Nützel, M., Oberländer-Hayn, S., Ruhnke, R., Runde, T., Sander, R., Scharffe, D., and Zahn, A.: Earth System Chemistry integrated Modelling (ESCiMo) with the Modular Earth Submodel System (MESSy) version 2.51, Geosci. Model Dev., 9, 1153–1200, doi:10.5194/gmd-9-1153-2016, http://www.geosci-model-dev.net/9/1153/2016/, 2016.

Kerkweg, A., Sander, R., Tost, H., and Jöckel, P.: Technical note: Implementation of prescribed (OFFLEM), calculated (ONLEM), and pseudo-emissions (TNUDGE) of chemical species in the Modular Earth Submodel System (MESSy), Atmos. Chem. Phys., 6, 3603–3609, doi:10.5194/acp-6-3603-2006, http://www.atmos-chem-phys.net/6/3603/2006/, 2006.

Koffi, B., Szopa, S., Cozic, A., Hauglustaine, D., and van Velthoven, P.: Present and future impact of aircraft, road traffic and shipping emissions on global tropospheric ozone, Atmos. Chem. Phys., 10, 11 681–11 705, doi:10.5194/acp-10-11681-2010, http://www.atmos-chem-phys.net/10/11681/2010/, 2010.

Lawrence, M. G. and Crutzen, P. J.: Influence of NOx emissions from ships on tropospheric photochemistry and climate, Nature, 402, 167–170, 1999.

Lelieveld, J. and Dentener, F. J.: What controls tropospheric ozone?, J. Geophys. Res. Atmos., 105, 3531–3551, doi:10.1029/1999JD901011, http://dx.doi.org/10.1029/1999JD901011, 2000.

Matthes, S., Grewe, V., Sausen, R., and Roelofs, G.-J.: Global impact of road traffic emissions on tropospheric ozone, Atmos. Chem. Phys., 7, 1707–1718, doi:10.5194/acp-7-1707-2007, http://www.atmos-chem-phys.net/7/1707/2007/, 2007.

Monks, P. S.: Gas-phase radical chemistry in the troposphere, Chem. Soc. Rev., 34, 376–395, doi:10.1039/B307982C, http://dx.doi.org/10.1039/B307982C, 2005.

Monks, P. S., Archibald, A. T., Colette, A., Cooper, O., Coyle, M., Derwent, R., Fowler, D., Granier, C., Law, K. S., Mills, G. E., Stevenson, D. S., Tarasova, O., Thouret, V., von Schneidemesser, E., Sommariva, R., Wild, O., and Williams, M. L.: Tropospheric ozone and its precursors from the urban to the global scale from air quality to short-lived climate forcer, Atmos. Chem. Phys., 15, 8889–8973, doi:10.5194/acp-15-8889-2015, http://www.atmos-chem-phys.net/15/8889/2015/, 2015.

Myhre, G., Shine, K., Rädel, G., Gauss, M., Isaksen, I., Tang, Q., Prather, M., Williams, J., van Velthoven, P., Dessens, O., Koffi, B., Szopa, S., Hoor, P., Grewe, V., Borken-Kleefeld, J., Berntsen, T., and Fuglestvedt, J.: Radiative forcing due to changes in ozone and methane caused by the transport sector, Atmospheric Environment, 45, 387–394, doi:http://doi.org/10.1016/j.atmosenv.2010.10.001, http://www.sciencedirect.com/science/article/pii/S1352231010008629, 2011.

Myhre, G., Shindell, D., Breéon, F.-M., Collins, W., Fuglestvedt, J., Huang, J., Koch, D., Lamarque, J.-F., Lee, D., Mendoza, B., Nakajima, T., Robock, A., Stephens, G., Takemura, T., and Zhang, H.: Anthropogenic and Natural Radiative Forcing, pp. 659–740, doi:10.1017/CBO9781107415324.018, www.climatechange2013.org, 2013.

Naik, V., Voulgarakis, A., Fiore, A. M., Horowitz, L. W., Lamarque, J.-F., Lin, M., Prather, M. J., Young, P. J., Bergmann, D., Cameron-Smith, P. J., Cionni, I., Collins, W. J., Dalsøren, S. B., Doherty, R., Eyring, V., Faluvegi, G., Folberth, G. A., Josse, B., Lee, Y. H., MacKenzie, I. A., Nagashima, T., van Noije, T. P. C., Plummer, D. A., Righi, M., Rumbold, S. T., Skeie, R., Shindell, D. T., Stevenson, D. S., Strode, S., Sudo, K., Szopa, S., and Zeng, G.: Preindustrial to present-day changes in tropospheric hydroxyl radical and methane lifetime from the Atmospheric Chemistry and Climate Model Intercomparison Project (ACCMIP), Atmospheric Chemistry and Physics, 13, 5277–5298, doi:10.5194/acp-13-5277-2013, http://www.atmos-chem-phys.net/13/5277/2013/, 2013.

Niemeier, U., Granier, C., Kornblueh, L., Walters, S., and Brasseur, G. P.: Global impact of road traffic on atmospheric chemical composition and on ozone climate forcing, J. Geophys. Res. Atmos., 111, doi:10.1029/2005JD006407, http://dx.doi.org/10.1029/2005JD006407, 2006.

Reis, S., Simpson, D., Friedrich, R., Jonson, J., Unger, S., and Obermeier, A.: Road traffic emissions ? predictions of future contributions to regional ozone levels in Europe, Atmospheric Environment, 34, 4701–4710, doi:http://dx.doi.org/10.1016/S1352-2310(00)00202-8, http://www.sciencedirect.com/science/article/pii/S1352231000002028, 2000.

Riahi, K., Grübler, A., and Nakicenovic, N.: Scenarios of long-term socio-economic and environmental development under climate stabilization, Technological Forecasting and Social Change, 74, 887 – 935, doi:http://dx.doi.org/10.1016/j.techfore.2006.05.026, http://www.sciencedirect.com/science/article/pii/S0040162506001387, greenhouse Gases - Integrated Assessment, 2007.

Riahi, K., Rao, S., Krey, V., Cho, C., Chirkov, V., Fischer, G., Kindermann, G., Nakicenovic, N., and Rafaj, P.: RCP 8.5—A scenario of comparatively high greenhouse gas emissions, Climatic Change, 109, 33, doi:10.1007/s10584-011-0149-y, http://dx.doi.org/10.1007/s10584-011-0149-y, 2011.

Righi, M., Hendricks, J., and Sausen, R.: The global impact of the transport sectors on atmospheric aerosol: simulations for year 2000 emissions, Atmospheric Chemistry and Physics, 13, 9939–9970, doi:10.5194/acp-13-9939-2013, http://www.atmos-chem-phys.net/13/9939/2013/, 2013.

Roeckner, E., Brokopf, R., Esch, M., Giorgetta, M., Hagemann, S., Kornblueh, L., Manzini, E., Schlese, U., and Schulzweida, U.: Sensitivity of Simulated Climate to Horizontal and Vertical Resolution in the ECHAM5 Atmosphere Model, J. Climate, 19, 3771–3791, doi:10.1175/jcli3824.1, http://dx.doi.org/10.1175/jcli3824.1, 2006.

Sander, R., Baumgaertner, A., Gromov, S., Harder, H., Jöckel, P., Kerkweg, A., Kubistin, D., Regelin, E., Riede, H., Sandu, A., Taraborrelli, D., Tost, H., and Xie, Z.-Q.: The atmospheric chemistry box model CAABA/MECCA-3.0, Geosci. Model Dev., 4, 373–380, doi:10.5194/gmd-4-373-2011, http://www.geosci-model-dev.net/4/373/2011/, 2011.

Schumann, U. and Huntrieser, H.: The global lightning-induced nitrogen oxides source, Atmos. Chem. Phys., 7, 3823–3907, doi:10.5194/acp-7-3823-2007, http://www.atmos-chem-phys.net/7/3823/2007/, 2007.

Seinfeld, J. H. and Pandis, S. N.: Atmospheric Chemistry and Physics: From Air Pollution to Climate Change, Wiley, 2006.

Stevenson, D. S., Dentener, F. J., Schultz, M. G., Ellingsen, K., van Noije, T. P. C., Wild, O., Zeng, G., Amann, M., Atherton, C. S., Bell, N., Bergmann, D. J., Bey, I., Butler, T., Cofala, J., Collins, W. J., Derwent, R. G., Doherty, R. M., Drevet, J., Eskes, H. J., Fiore, A. M., Gauss, M., Hauglustaine, D. A., Horowitz, L. W., Isaksen, I. S. A., Krol, M. C., Lamarque, J.-F., Lawrence, M. G., Montanaro, V., Müller, J.-F., Pitari, G., Prather, M. J., Pyle, J. A., Rast, S., Rodriguez, J. M., Sanderson, M. G., Savage, N. H., Shindell, D. T., Strahan, S. E., Sudo, K., and Szopa, S.: Multimodel ensemble simulations of present-day and near-future tropospheric ozone, J. Geophys. Res. Atmos., 111, doi:10.1029/2005JD006338, http://dx.doi.org/10.1029/2005JD006338, 2006.

Stuber, N., Sausen, R., and Ponater, M.: Stratosphere adjusted radiative forcing calculations in a comprehensive climate model, Theor. Appl. Climatol., 68, 125–135, 2001.

Tagaris, E., Sotiropoulou, R. E. P., Gounaris, N., Andronopoulos, S., and Vlachogiannis, D.: Effect of the Standard Nomenclature for Air Pollution (SNAP) Categories on Air Quality over Europe, Atmosphere, 6, 1119, doi:10.3390/atmos6081119, http://www.mdpi.com/2073-4433/6/8/1119, 2015.

Tost, H., Jöckel, P., Kerkweg, A., Sander, R., and Lelieveld, J.: Technical note: A new comprehensive SCAVenging submodel for global atmospheric chemistry modelling, Atmos. Chem. Phys., 6, 565–574, doi:10.5194/acp-6-565-2006, http://www.atmos-chem-phys.net/6/565/2006/, 2006.

Uherek, E., Halenka, T., Borken-Kleefeld, J., Balkanski, Y., Berntsen, T., Borrego, C., Gauss, M., Hoor, P., Juda-Rezler, K., Lelieveld, J., Melas, D., Rypdal, K., and Schmid, S.: Transport impacts on atmosphere and climate: Land transport, Atmospheric Environment, 44, 4772–4816, doi:http://doi.org/10.1016/j.atmosenv.2010.01.002, http://www.sciencedirect.com/science/article/pii/S1352231010000099, transport Impacts on Atmosphere and Climate: The {ATTICA} Assessment Report, 2010.

Vinken, G. C. M., Boersma, K. F., Maasakkers, J. D., Adon, M., and Martin, R. V.: Worldwide biogenic soil NO_x emissions inferred from OMI NO_2 observations, Atmos. Chem. Phys., 14, 10 363–10 381, doi:10.5194/acp-14-10363-2014, http://www.atmos-chem-phys.net/14/10363/2014/, 2014.

von Kuhlmann, R., Lawrence, M. G., Pöschl, U., and Crutzen, P. J.: Sensitivities in global scale modeling of isoprene, Atmos. Chem. Phys., 4, 1–17, doi:10.5194/acp-4-1-2004, http://www.atmos-chem-phys.net/4/1/2004/, 2004.

Wild, O. and Prather, M. J.: Global tropospheric ozone modeling: Quantifying errors due to grid resolution, J. Geophys. Res. Atmos., 111, n/a–n/a, doi:10.1029/2005JD006605, http://dx.doi.org/10.1029/2005JD006605, d11305, 2006.

Williams, J., Hodnebrog, Ø., van Velthoven, P., Berntsen, T., Dessens, O., Gauss, M., Grewe, V., Isaksen, I., Olivié, D., Prather, M., and Tang, Q.: The influence of future non-mitigated road transport emissions on regional ozone exceedences at global scale, Atmospheric Environment, 89, 633 – 641, doi:https://doi.org/10.1016/j.atmosenv.2014.02.041, http://www.sciencedirect.com/science/article/pii/S135223101400137X, 2014.

World Health Organization: Health aspect of air pollution with particulate matter, ozone and nitrogen dioxide, World Health Organization, Bonn, 2003.

Wu, S., Duncan, B. N., Jacob, D. J., Fiore, A. M., and Wild, O.: Chemical nonlinearities in relating intercontinental ozone pollution to anthropogenic emissions, Geophys. Res. Lett., 36, n/a–n/a, doi:10.1029/2008GL036607, http://dx.doi.org/10.1029/2008GL036607, l05806, 2009.

Yienger, J. J. and Levy, H.: Global inventory of soil-biogenic NO x emissions, J. Geophys. Res., 100, 11,447–11,464, 1995.

Young, P. J., Archibald, A. T., Bowman, K. W., Lamarque, J.-F., Naik, V., Stevenson, D. S., Tilmes, S., Voulgarakis, A., Wild, O., Bergmann, D., Cameron-Smith, P., Cionni, I., Collins, W. J., Dalsøren, S. B., Doherty, R. M., Eyring, V., Faluvegi, G., Horowitz, L. W., Josse, B., Lee, Y. H., MacKenzie, I. A., Nagashima, T., Plummer, D. A., Righi, M., Rumbold, S. T., Skeie, R. B., Shindell, D. T., Strode, S. A., Sudo, K., Szopa, S., and Zeng, G.: Pre-industrial to end 21st century projections of tropospheric ozone from the Atmospheric Chemistry and Climate Model Intercomparison Project (ACCMIP), Atmos. Chem. Phys., 13, 2063–2090, doi:10.5194/acp-13-2063-2013, http://www.atmos-chem-phys.net/13/2063/2013/, 2013.